UCLA

· Department of Physics ·

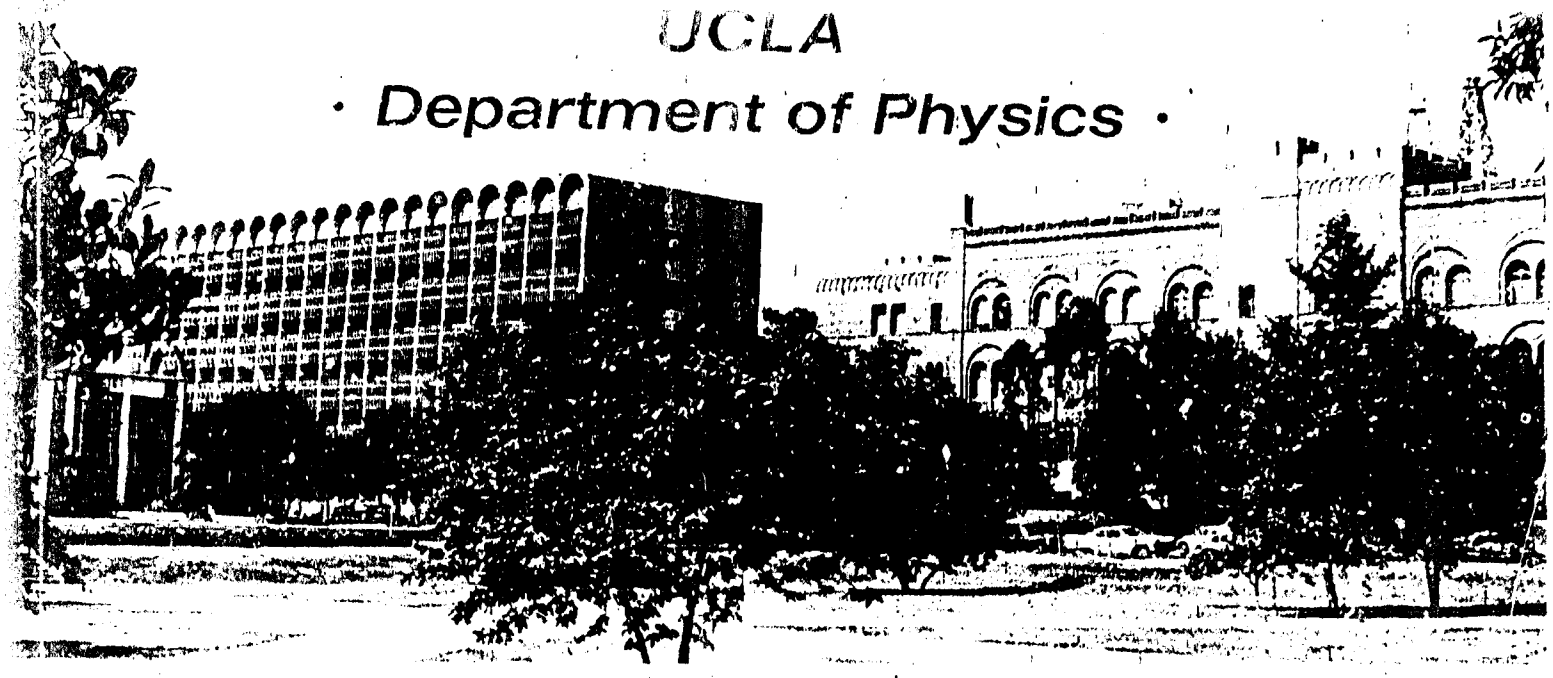

AD 744710

LOS ANGELES 90024

CALIFORNIA

Technical Report No. 34

June, 1972

Submitted by

I. Rudnick, Project Director

Hypersonic Attenuation in the Vicinity of the Superfluid Transition of Liquid Helium

by

Daniel E. Commins

Details of illustrations in this document may be better studied on microfiche

Office of Naval Research
Contract:
N00014-69-A-0200-4014
NR No. 384-302

Department of Physics
University of California
Los Angeles, Calif. 90024

UNCLASSIFIED
Security Classification

DOCUMENT CONTROL DATA - R & D

Security classification of title, body of abstract and indexing annotation must be entered when the overall report is classified

1 ORIGINATING ACTIVITY (Corporate author) University of California, Los Angeles	2a. REPORT SECURITY CLASSIFICATION Unclassified 2b. GROUP

3 REPORT TITLE

Hypersonic Attenuation in the Vicinity of the Superfluid Transition of Liquid Helium

4 DESCRIPTIVE NOTES (Type of report and inclusive dates)

5 AUTHOR(S) (First name, middle initial, last name)

Daniel E. Commins

6. REPORT DATE	7a. TOTAL NO. OF PAGES	7b. NO OF REFS
June 1972	90	52

8a. CONTRACT OR GRANT NO	9a. ORIGINATOR'S REPORT NUMBER(S)
N00014-69-A-0200-4014 NR 384-302 b. PROJECT NO. c. d.	Technical Report No. 34 9b. OTHER REPORT NO(S) (Any other numbers that may be assigned this report)

10 DISTRIBUTION STATEMENT

DISTRIBUTION OF THIS DOCUMENT IS UNLIMITED

11 SUPPLEMENTARY NOTES	12. SPONSORING MILITARY ACTIVITY

13 ABSTRACT The relative ultrasonic attenuation in liquid helium at 1 GHz has been measured in the critical region with a fixed path interferometer. The sample was isolated from the main bath by a vacuum and the amplitude of the transmitted sound wave was measured while the temperature of the sample was made to drift at rates as slow as 3×10^{-6}°K sec^{-1}. The attenuation is found to have a very large non-singular peak of about 2500/cm^{-2} with its maximum at 3.26± .20 m°K below the lambda point. After the contribution of viscous and thermal losses to the attenuation has been subtracted, the temperature dependence of the critical attenuation is found to vary approximately as $|T_p - T|^{-1/2}$ on both sides of T_p, the temperature of the peak. The attenuation peak cannot be explained by the Landau-Khalatnikov theory, and processes other than the decay of first into second sound must be considered. These results are in substantial agreement with earlier results[1] but locate the peak with much greater reliability.

(1) J.S. Imai and I. Rudnick, Phys. Rev. Lett. 22, 694 (1969)

DD FORM 1 NOV 65 1473 (PAGE 1)

S/N 0101-807-6801

UNCLASSIFIED
Security Classification

14 KEY WORDS	LINK A		LINK B		LINK C	
	ROLE	WT	ROLE	WT	ROLE	WT
LIQUID HELIUM						
FIRST SOUND						
ATTENUATION						
CRITICAL PHENOMENA						
PHASE TRANSITION						
HYPERSONIC						
SUPERFLUID						

TABLE OF CONTENTS

LIST OF FIGURES

LIST OF TABLES

LIST OF SYMBOLS

A	Signal Amplitude
C_p	Specific Heat for Constant Pressure
C_S	Specific Heat Under Saturated Vapor Pressure
C_V	Specific Heat for Constant Volume
He	Helium
He I	Helium Above the Lambda Transition
He II	Helium Below the Lambda Transition
He^3, He^4	Helium Isotopes
K_T	Isothermal Compressibility
k	Boltzmann Constant
k_l	Wave Vector
k_1	Light Scattering Wave Vector
k_n	Neutron Scattering Wave Vector
k_s	Ultrasonic Wave Vector
<M>	Magnetization
<p>	Order Parameter
P	Pressure
S	Entropy per Unit Mass
S_s	Entropy of the Superfluid per Unit Mass
s	Ising Spin
t	Time
T	Temperature
T_λ	Lambda Temperature for He^4
T_c	Critical Temperature
T_p	Temperature of the Attenuation Peak
u_1	Velocity of First Sound
u_2	Velocity of Second Sound
u_4	Velocity of Fourth Sound
u_o	Zero Frequency Limit of u_1
u_∞	Infinite Frequency Limit of u_1
V_A	Acoustical Signal Amplitude

V_E	Electrical Signal Amplitude
v_n	Normal Fluid Velocity
v_s	Superfluid Velocity
α	Attenuation of First Sound
α_{abs}	Absolute Attenuation
α_c	Classical Attenuation
α_{KC}	Khalatnikov-Chernikova Attenuation
α_{LK}	Landau-Khalatnikov Attenuation
α_{total}	Total Attenuation
α_κ	Attenuation Due to Thermal Losses
α_η	Attenuation Due to Viscous Losses
β_p	Isobaric Coefficient of Thermal Expansion
β_{sat}	Coefficient of Thermal Expansion Under Saturated Vapor Pressure
β_T	Isothermal Compressibility Coefficient
γ	Ratio of C_p and C_V
δ	Acoustical Path
Δ	Complex Gap Parameter
ϵ	$(T-T_\lambda)/T_\lambda$, Normalized Temperature
ζ	Volume Viscosity
η	Shear Viscosity
η_n	Shear Viscosity for the Normal Fluid
η_s	Shear Viscosity for the Superfluid
κ	Heat Conductivity
λ	Lambda (Transition)
ν	Frequency
ν_A	Interatomic Collision Frequency
ξ	Correlation Length
ρ	Mass Density
ρ_c	Critical Density
ρ_n	Normal Fluid Density
ρ_s	Superfluid Density
τ	Relaxation Time
τ_{eff}	Effective Cut-off Relaxation Time

τ_1	ξ/u_1
τ_2	ξ/u_2
τ_{pr}	Phonon-Roton Relaxation Time
$\tau_{3\rightarrow 2}$	Five-Phonon Process Relaxation Time
ψ	Wave Function
ω	Angular Frequency

ACKNOWLEDGMENTS

I wish to thank Professor Isadore Kudnick for his guidance and for his support and friendship.

I also want to express my appreciation to the faculty members who have accepted to sit on my committee and to Professors Joachim Frenkiel, Vern O. Knudsen, Moises Levy, David S. Saxon, Giovan G. Natale, and, in particular, Michael Woolf and Etienne Guyon for their interest and warm encouragements.

I naturally owe thanks to the faculty and staff members of the UCLA Physics Department and to the members, past and present, of the Acoustics Group who gave me a helping hand many times.

Finally, I wish to thank Pedro Oillataguerre and Trudi Bomba who have advised me wisely and have honored me with their friendship and Donald Perry for assisting with some of the measurements.

Merci!

ABSTRACT OF THE DISSERTATION

Hypersonic Attenuation in the Vicinity of the

Superfluid Transition of Liquid Helium

by

Daniel Edwin Commins

Doctor of Philosophy in Physics

University of California, Los Angeles, 1972

Professor Isadore Rudnick, Chairman

The attenuation of first sound waves has been measured in liquid helium at a frequency of 1 GHz. Absolute measurements were performed with a variable path interferometer for temperatures extending from 1.1°K to 4.2°K. The results confirm those obtained earlier by the same method and those obtained from the Brillouin spectrum of scattered light. They can be described in terms of three regions: a) the normal fluid region above 2.3°K where the attenuation is attributed to the classical losses associated with viscosity and thermal conduction; b) the critical region between 2.0°K and 2.3°K, where the attenuation has a sharp peak occurring near T_λ; c) the superfluid region where the attenuation shows a broad maximum centered at 1.5°K and which is in agreement with the Khalatnikov-Chernikova theory. When the 1 GHz results are compared with the Brillouin scattering results, which vary in frequency from 556 MHz to 768 MHz, it is found that the attenuation scales as ω^2 over the whole temperature range with the possible exception of the data below 1.5°K and in the immediate vicinity of T_λ.

In the critical region, extending from 2.0°K to 2.3°K, more accurate attenuation measurements were performed with a fixed path interferometer. The helium sample was isolated from the helium bath and its temperature was allowed to drift as slowly as 3×10^{-6} °K sec^{-1}.

The attenuation exhibits a sharp maximum in the region of the lambda transition; the largest value is about 2500 cm^{-1} and occurs at a temperature $T_\lambda - T_p = 3.26 \pm 0.20$ millidegrees, which was found to be independent of the power of the input signal.

After subtracting the classical attenuation due to viscous and thermal losses, the temperature dependence has been determined on both sides of the peak by fitting a power law of the form

$$\alpha = a/|T_p - T|^n$$

if the immediate vicinity of the maximum is excluded.

For $T > T_\lambda$, $\bar{n} = 0.49 \pm 0.06$ and $\bar{a} = 232$ $(°K)^n/cm$.

For $T < T_\lambda$, $\bar{n} = 0.51 \pm 0.05$ and $\bar{a} = 152$ $(°K)^n/cm$.

The contribution of the Landau-Khalatnikov relaxation mechanism at a frequency of 1 GHz is a peak, centered 94 m°K below T_λ, of only about 180 cm^{-1}; therefore the present results cannot be explained by such a process. The other existing theories have been surveyed and no satisfactory explanation of the sharp attenuation peak has been found.

I. INTRODUCTION

The aim of this investigation is to study the behavior of hypersonic waves in liquid helium in the vicinity of its lambda transition. To introduce the subject, the general properties of liquid helium will be reviewed and different types of wave propagation will be described. To familiarize the reader with the quantities used throughout this work, the two fluid model of helium and the lambda transition will be discussed. Finally, the relevant experimental results concerning the absorption of ordinary sound in liquid helium will be reviewed.

1.1 Thermal Properties of Liquid He^4

Two stable isotopes of helium can be found: He^3 and He^4; in the present work only the latter will be considered. The phase diagram in the P-T plane for He^4 is shown in Fig. 1. It exhibits many interesting features of this extraordinary liquid.

In contrast with the phase diagram of an ordinary liquid, it does not show a triple point where the substance can be present at equilibrium in three states: solid, liquid and vapor. Another interesting feature is that helium can exist in the liquid state down to 0°K and no other substance can: the pressure which is required at absolute zero to solidify the liquid is approximately 25 atm., which indicates that the interatomic forces are very weak and the zero-point energy very large. Another manifestation of the same characteristics is the low critical point.

The so-called lambda line separates the two liquid phases of helium. On the high temperature side, where it is named liquid He I, helium be-

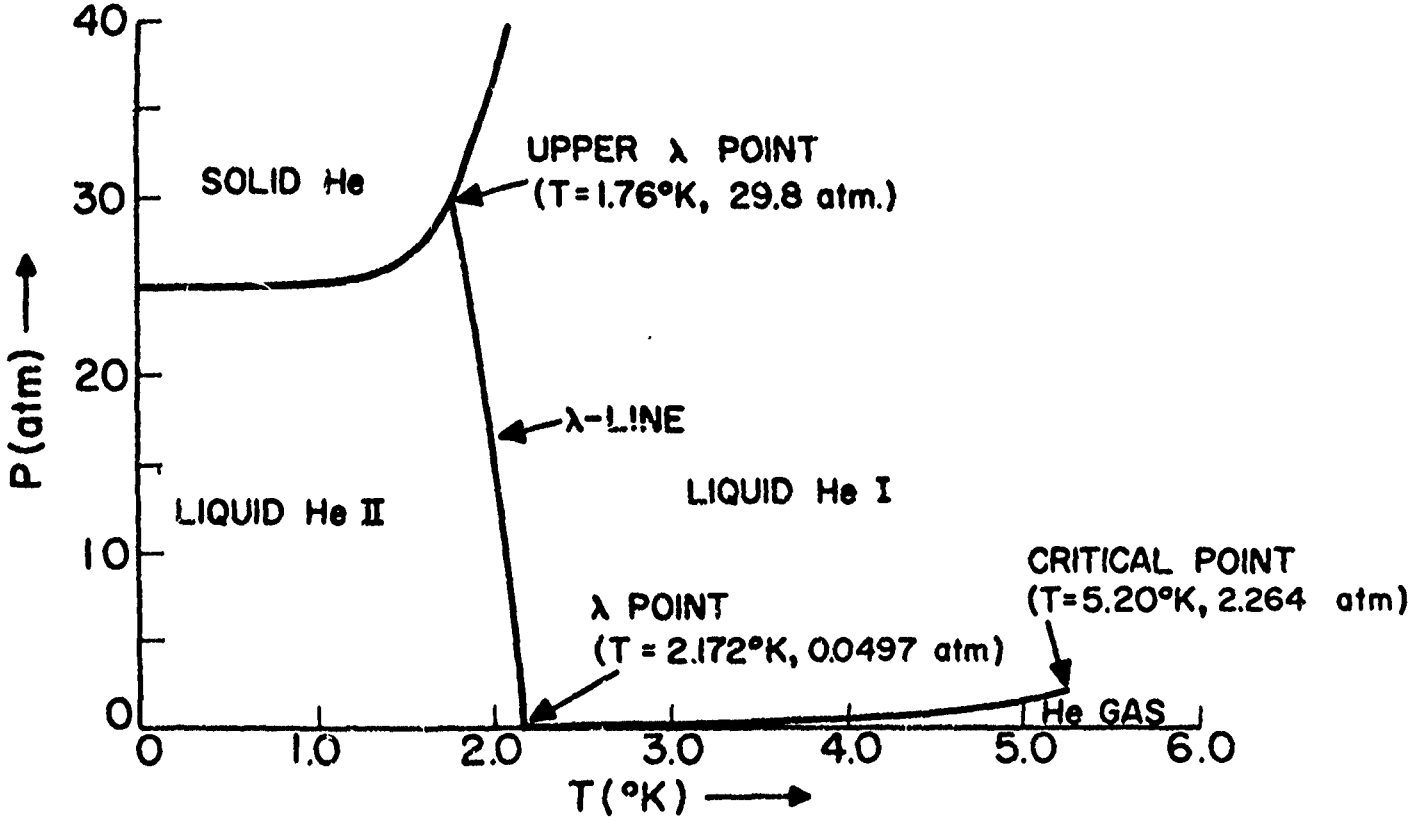

FIGURE 1.

THE PHASE DIAGRAM OF HELIUM-4 IN THE P-T PLANE

haves as an ordinary liquid, except close to the transition, while on the low side, that of liquid He II, helium exhibits its superfluid behavior; it is the region where quantum effects become macroscopic.

The lambda transition is not accompanied by a latent heat and the quantities which are first derivatives of the Gibbs free energy, the entropy and density,[1] (Fig. 2), are continuous across the transition. Higher order derivatives are affected by the transition. For instance, the specific heat, along the vapor pressure curve, becomes large in the vicinity of the lambda transition on both sides (Fig. 3).[2] Being shaped like the Greek letter lambda, it suggested the name of the transition. A semi-logarithmic plot[3] (Fig. 4) shows that the specific heat, at the saturated vapor pressure, has a logarithmic singularity at T_λ.

1.2 Wave Propagation in Liquid He^4

Above the superfluid transition, the only propagating mode is the ordinary pressure-density sound wave. Below the transition, several types of wave motion can propagate: they are called "sound," even though they are not all acoustic waves, and they are numbered from one to four.

Ordinary sound, the adiabatic propagation of a pressure density excursion, is called "first sound" and its velocity is given classically by

$$u_1^2 = \left(\frac{\partial P}{\partial \rho}\right)_S = \frac{\gamma}{\rho \beta_T} \tag{1}$$

where $\gamma = C_p/C_v$ is the ratio of the specific heats at constant pressure and at constant volume, ρ is the density, and β_T is the

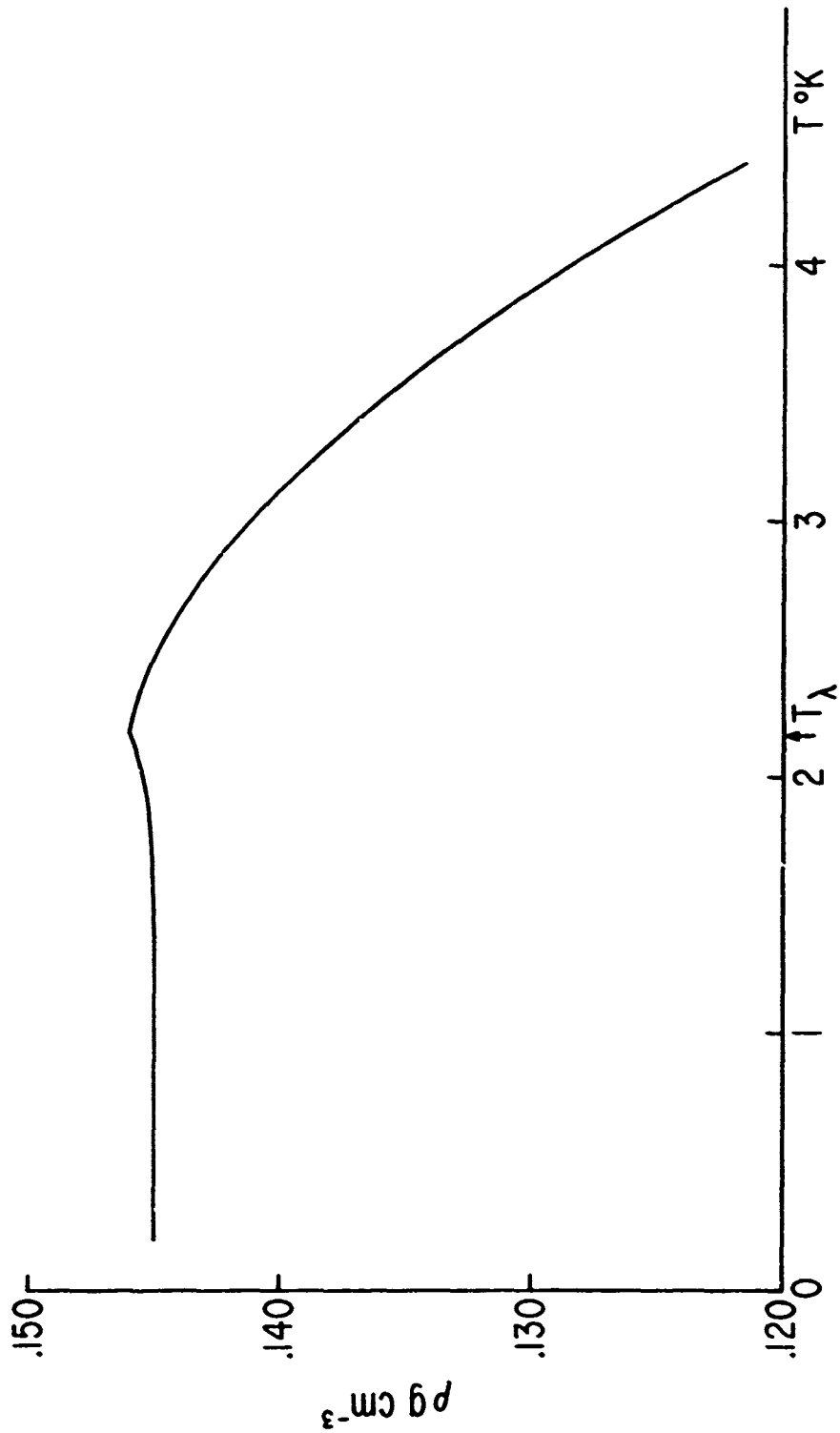

FIGURE 2.
DENSITY vs. TEMPERATURE

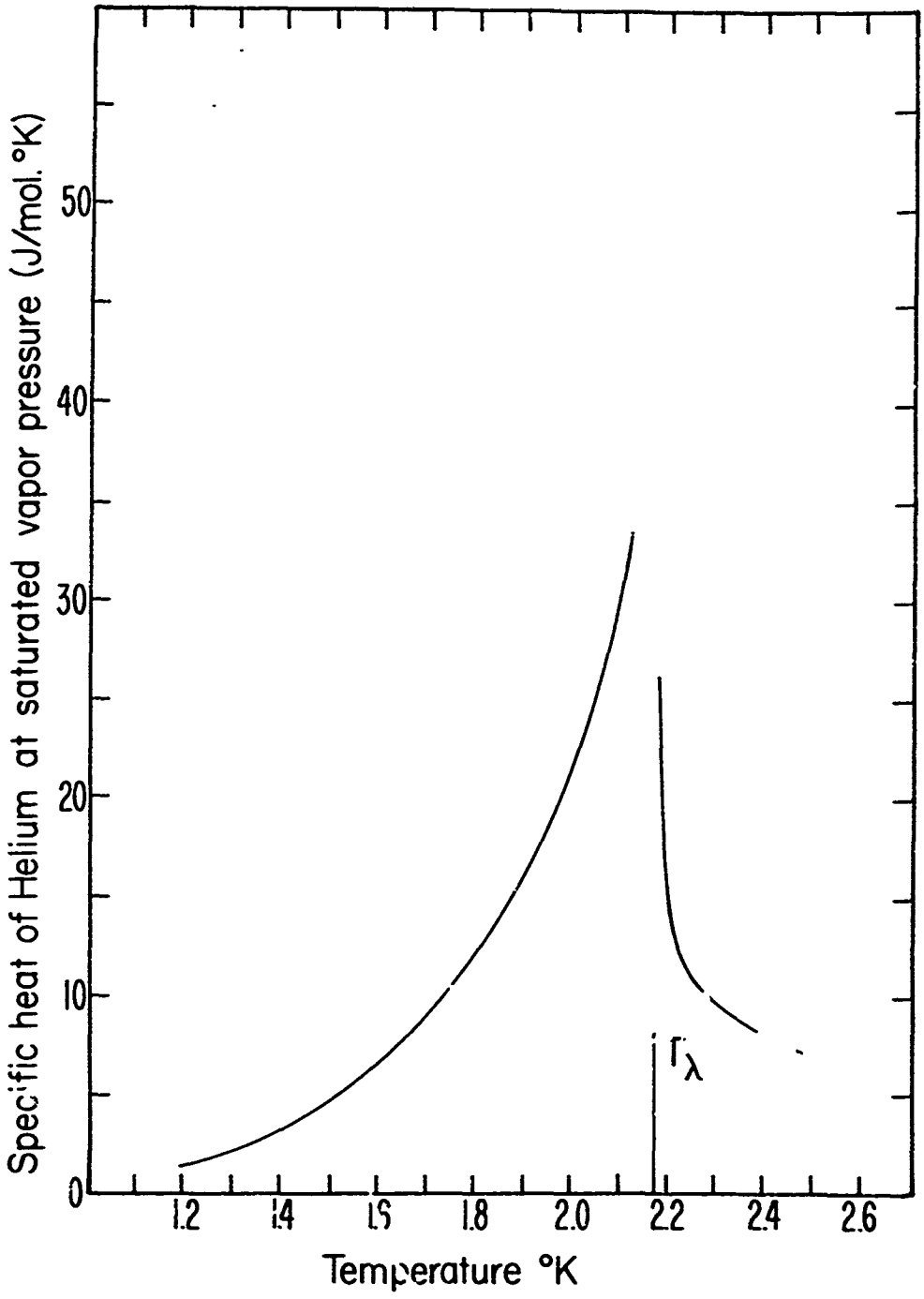

FIGURE 3.

SPECIFIC HEAT OF He^4

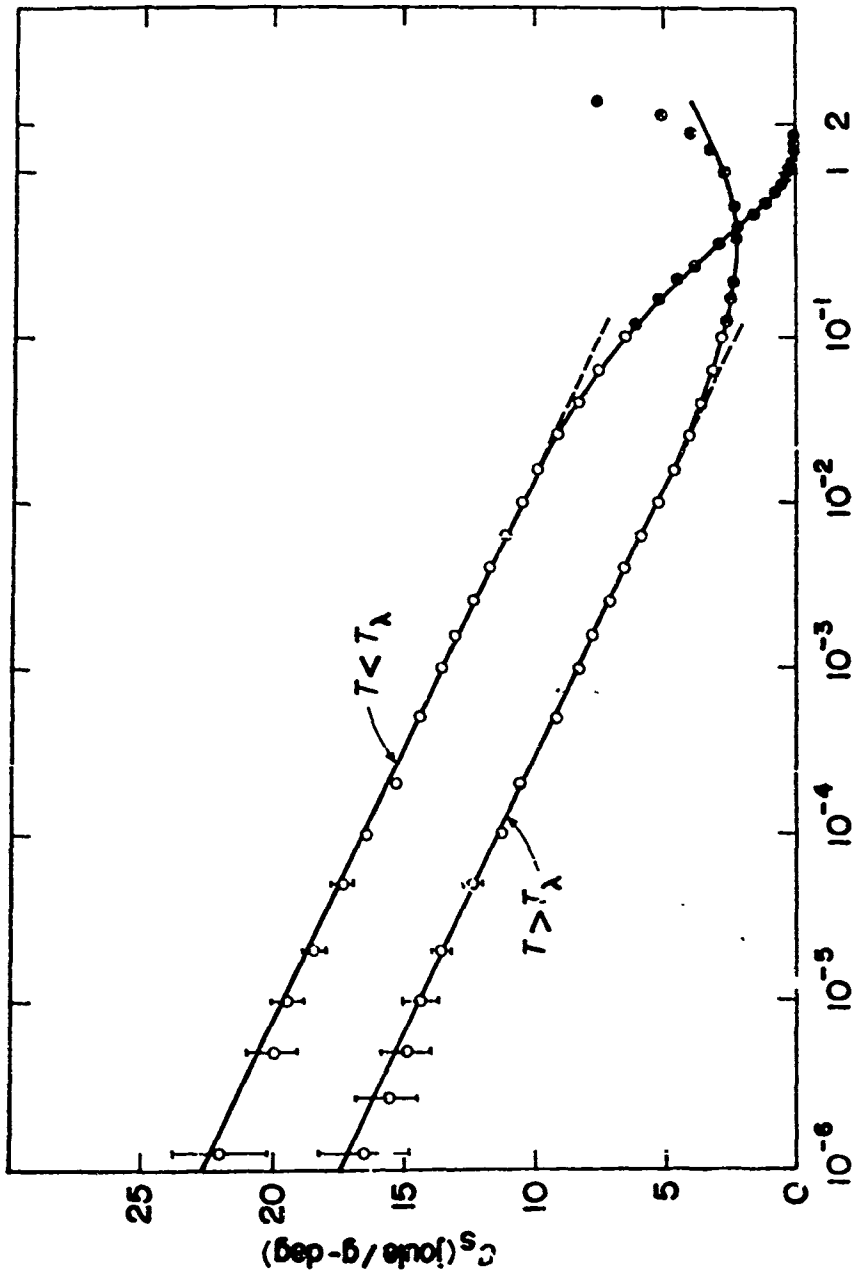

FIGURE 4.

SPECIFIC HEAT NEAR THE LAMBDA POINT

isothermal compressibility coefficient.

As shown in Fig. 5, the velocity of first sound is almost constant as a function of temperature except for a cusp around the transition.

"Second sound"[4,5] is a temperature wave, that is, an entropy-temperature disturbance; a temperature pulse, generated by a heater at one point, can be detected undistorted at another. The temperature dependence of the second sound velocity u_2 is complex, as can be seen in Fig. 5.

In restricted geometries, other types of waves may exist. "Third sound"[6,7] is the propagation of surface waves on a helium film. "Fourth sound"[6,8,9] is a thermal wave propagating in a narrow channel, and its velocity is given by a combination of u_1 and u_2. Figure 5 shows the temperature dependence of u_4, the velocity of fourth sound.

1.3 The Two-Fluid Model of He II

To explain the behavior of He^4 below the lambda transition, Tisza[10] proposed to study the liquid as if it were composed of two interpenetrating fluids: the normal fluid which exhibits the features of an ordinary liquid with density ρ_n and velocity $\vec{v}_n$, and the superfluid with density ρ_s and velocity $\vec{v}_s$. The total density is the sum of the particle densities

$$\rho = \rho_n + \rho_s \tag{2}$$

The temperature dependence of ρ_n/ρ and ρ_s/ρ under saturated vapor pressure is shown in Fig. 6.

The two fluid idea emerged to explain the discrepancy between

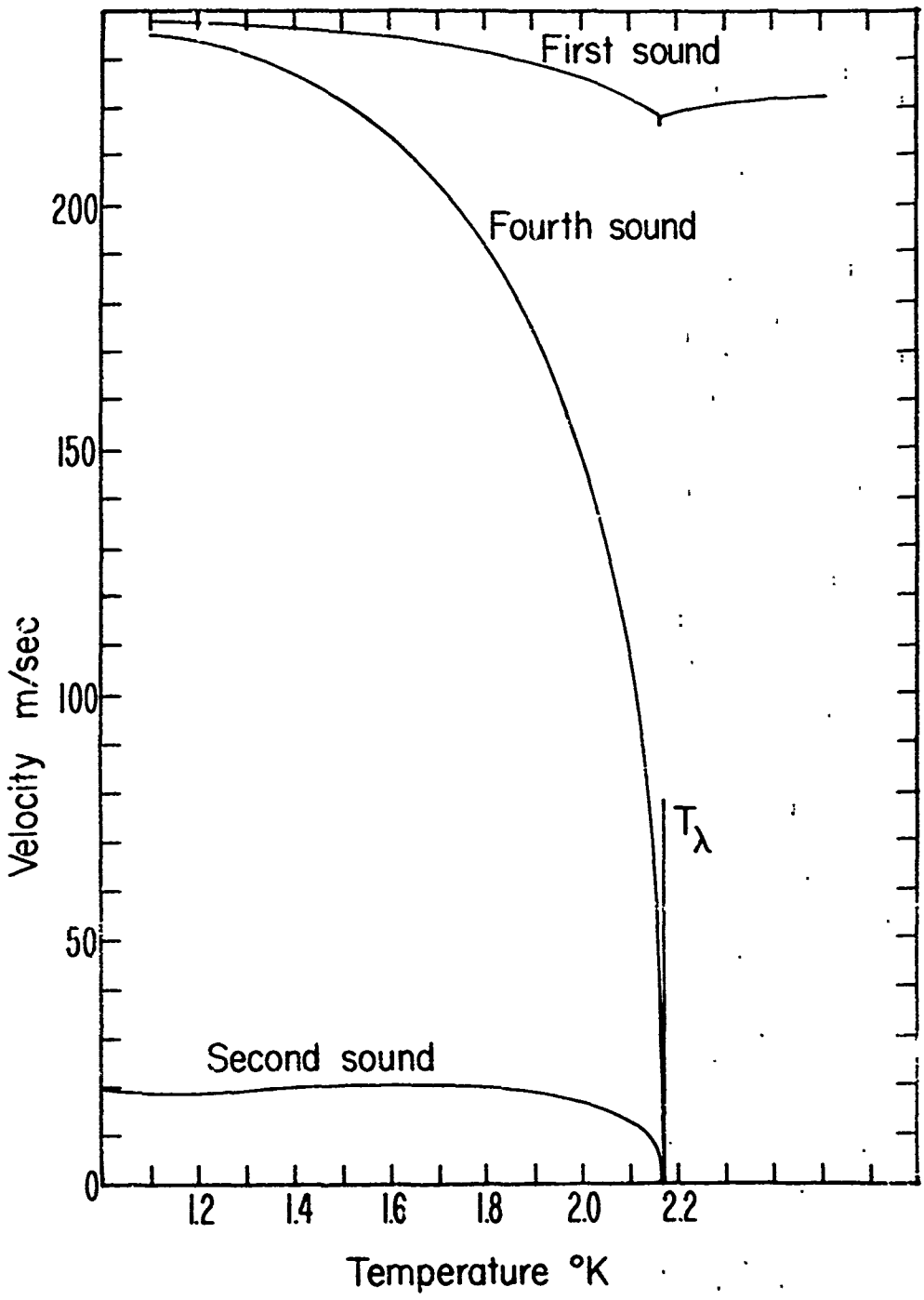

FIGURE 5.

FIRST, SECOND AND FOURTH SOUND VELOCITIES

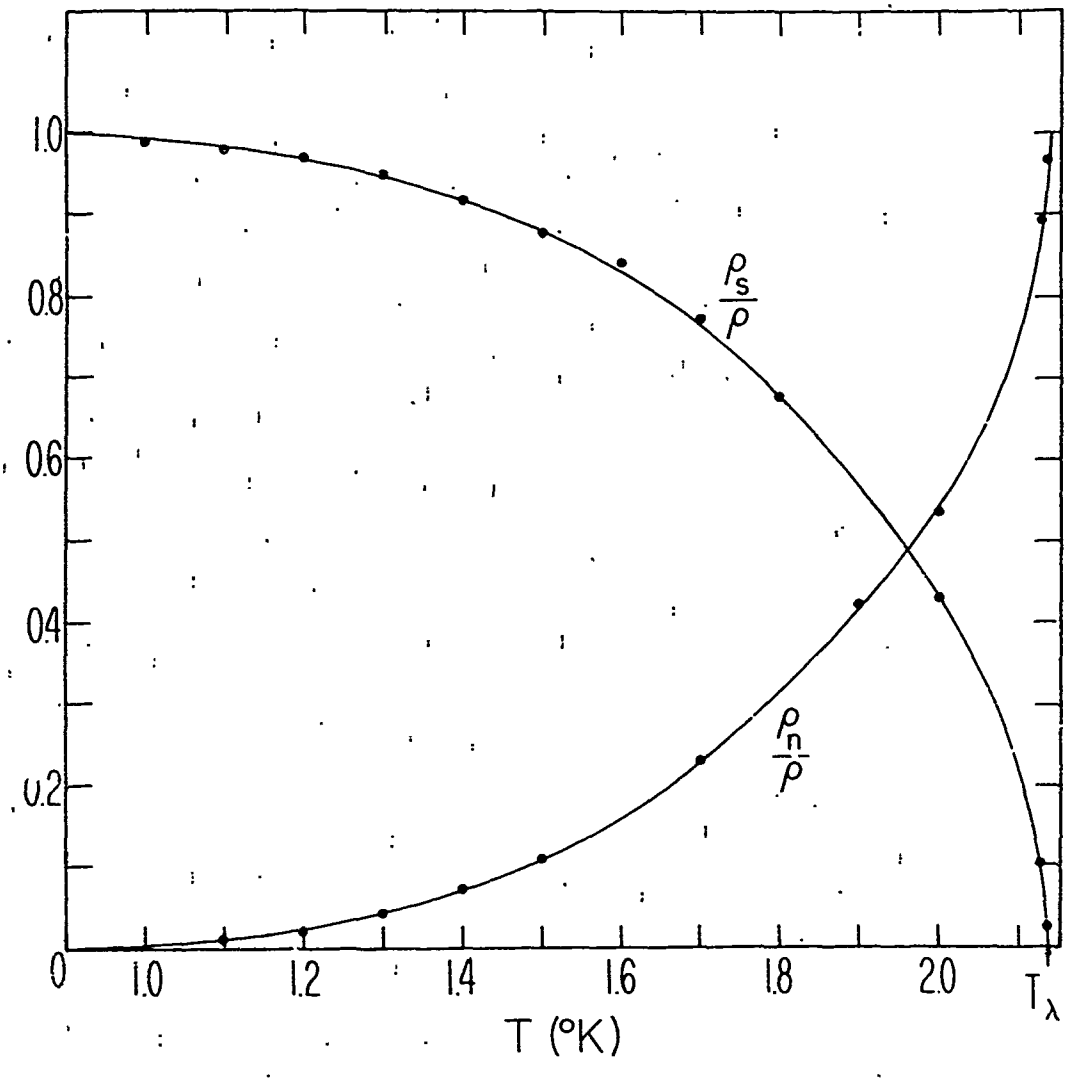

FIGURE 6.

THE NORMAL AND SUPERFLUID FRACTIONS OF LIQUID HELIUM-II[14]

experimental determinations of the viscosity. When measuring the flow of He^4 below T_λ through narrow capillaries,[11,12] it was found that the viscosity became immeasurably small. When measured by the rotating disk method,[13] the viscosity, even though decreasing with temperature, is found to be of the same order as the viscosity of He I. The two fluid model clarifies this paradox: in the capillary method, only the "non-viscous" superfluid flows through, while in the rotating disk method part of the normal fluid gets dragged by the rotating disk, causing viscous losses.

In addition to being assumed non-viscous, the superfluid does not carry entropy:

$$\eta_s = 0 \qquad S_s = 0 \tag{3}$$

The superfluid equation for low velocities in the absence of external forces is[15]

$$\rho_s \frac{\partial \vec{v}_s}{\partial t} = -\frac{\rho_s}{\rho} \vec{\nabla} P + \rho_s S \vec{\nabla} T \tag{4}$$

and the normal fluid equation is, under the same conditions,

$$\rho_n \frac{\partial \vec{v}_n}{\partial t} = -\frac{\rho_n}{\rho} \vec{\nabla} P - \rho_s S \vec{\nabla} T + \eta_n \vec{\nabla} \times \vec{\nabla} \times \vec{v}_n \tag{5}$$

where S is the entropy per unit mass, η_n is the coefficient of shear viscosity of the normal fluid, P is the pressure, and T is the temperature. The last two equations show the duality between the influence of a thermal gradient and a pressure gradient on the fluid.

To complete the set of equations, one expresses the laws of conser-

vation of mass and entropy:

$$\frac{\partial \rho}{\partial t} = - \vec{\nabla} \cdot (\rho_s \vec{v}_s + \rho_n \vec{v}_n) \tag{6}$$

$$\frac{\partial (\rho S)}{\partial t} = - \vec{\nabla} \cdot (\rho S \vec{v}_n) \tag{7}$$

From Eqs. (2) - (7), the modes of propagation which are of interest in this study can be derived. First sound, in which the normal fluid and the superfluid move in phase

$$\vec{v}_n = \vec{v}_s \tag{8}$$

propagates with a velocity

$$u_1 = \left(\frac{\partial P}{\partial \rho}\right)^{1/2} \tag{9}$$

First sound, present below and above the transition, remains finite and continuous through the lambda point. The zero frequency limit of its velocity, at its minimum which occurs at T_λ, is u_o = 217 m/sec.

Second sound, present only in the He II phase, is a real propagating mode and not a simple diffusion wave. The normal fluid and the superfluid move out of phase, with

$$\rho_s \vec{v}_s + \rho_n \vec{v}_n = 0 \tag{10}$$

Its velocity is given by

$$u_2 = \left(\frac{\rho_s}{\rho_n} \frac{S^2 T}{C_p}\right)^{1/2} \tag{11}$$

and is plotted in Fig. 5. u_2 continuously goes to zero as the transition is approached since ρ_s goes to zero and C_p has a singularity at T_λ.

1.4 The Lambda Transition

The lambda transition of liquid helium is only one example of the phase transitions which can be described in terms of an order parameter that is a measure of the symmetry of the system in the vicinity of the transition temperature.[16]

Table I lists some transitions of order higher than one and the order parameter <p> associated with each of them.[17] The order parameter may have a zero average value in the disordered phase, that is, above the transition, and must be non-zero in the ordered phase below the transition.

In the vicinity of the lambda transition, the singular behavior of thermodynamic quantities is attributed to long-range fluctuations of the order parameter. The characteristic length ξ of these fluctuations is assumed to vary as some power of

$$\varepsilon^{-1} = \left| 1 - \frac{T}{T_\lambda} \right|^{-1} \qquad (12)$$

and diverges as T approaches T_λ.

Landau studied the thermodynamics of second order phase transitions by expressing the chemical potential as a function of three variables: the pressure P, the temperature T, and the order parameter. In the neighborhood of the transition, he expands the chemical potential as a power series of the order parameter; by studying the derivatives of this function with respect to temperature it is possible to determine the temperature dependence of the order parameter and the discontinuity of the specific heat C_p. In the particular case of liquid helium, this

TABLE I:

Partial List of Phase Transitions and Their Order Parameter $\langle p \rangle$.[17]

Transition	Meaning of $\langle p \rangle$
Liquid - Gas	$\rho - \rho_c$
Ferromagnetic	Magnetization $\langle M \rangle$
Heisenberg Model Ferromagnet	Magnetization $\langle M \rangle$
Antiferromagnet	Sublattice Magnetization
Ising Model	Ising Spin s
Superconductors	Complex Gap Parameter Δ
Superfluid	Condensate Wave Function $\langle \psi \rangle$
Ferroelectric	Lattice Polarization
Phase Separation	Concentration

theory seems to fail because it does not take into account the effect of fluctuations which, near T_λ, may be large and lead to the singular behavior of C_p.

Static scaling laws[17,18] assume that the consequences of fluctuations can be attributed to the characteristic length ξ and that, within a critical region, singular thermodynamic quantities can be found to vary as some power of ε. The relations between these exponents as determined by the scaling laws have in many cases been corroborated by experimental results. However, some unexplained contradictions leave questionable the validity of the static scaling laws.

By assuming, in addition to a characteristic length, a characteristic reciprocal time or frequency, static scaling theory can be extended to phenomena exhibiting non-zero wave vectors $\vec{k}$ thereby becoming the dynamic scaling theory.[19,20]

At a given temperature, the characteristic length ξ defines several regions (Fig. 7): (I) the hydrodynamic region below T_λ ($T > T_\lambda$, $k\xi << 1$), (II) the critical region near T_λ ($k\xi >> 1$), (III) the hydrodynamic region above T_λ ($T > T_\lambda$, $k\xi << 1$).

The separation between critical and hydrodynamic behavior is indicated by the lines $k\xi = 1$.

This figure shows that while neutron scattering experiments deal with large wave-numbers k_n and hydrodynamics does not apply, for light scattering experiments characterized by very small wave numbers k_l hydrodynamics applies at almost all temperatures. For ultrasonic absorption experiments the relative width of the critical region can be adjusted by the choice of the frequency.

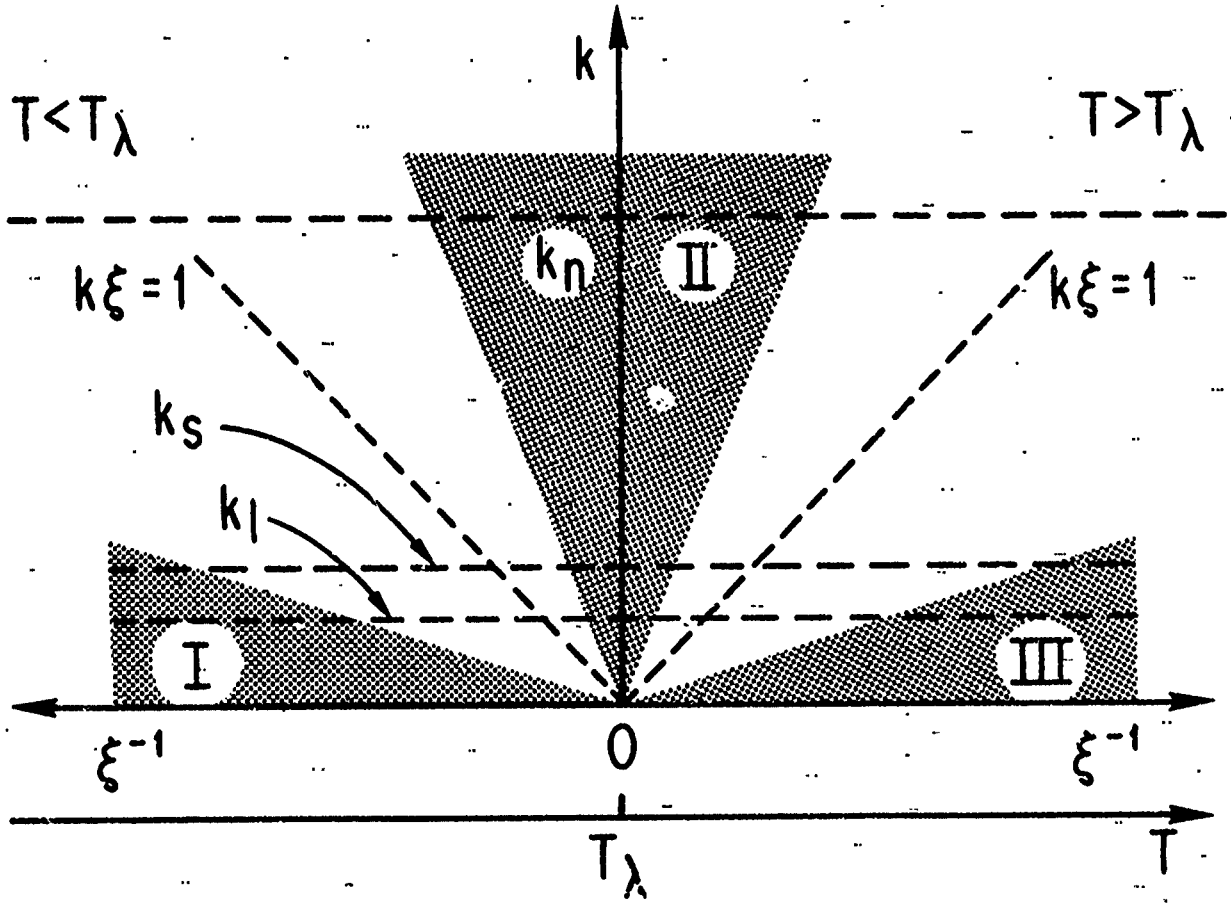

FIGURE 7.

SCHEMATIC PLOT OF THE WAVENUMBER k vs. THE RECIPROCAL CORRELATION LENGTH

The present study is an attempt to investigate the region for which $k\xi$ is not small; it must be pointed out, however, that, since little is known about ξ, the quantity $k\xi$ cannot be evaluated with certainty. It is nevertheless of interest to evaluate the attenuation of first sound at high frequencies, since some absorption processes might be enhanced while some others become insignificant.

1.5 History of First Sound Attenuation Near T_λ

The absorption of sound waves has been used extensively to investigate the properties of solids and fluids. Ultrasonic measurements, in particular, provide a rather complete tool for the study of phase transitions[21] since their static and dynamic properties can be probed. In a superfluid, moreover, due to the extraordinary thermal nature of the fluid, it is possible to approach the critical region more easily than in other substances.

The "anomalous" or "critical" attenuation in liquid helium near the lambda transition was first observed by Pellam and Squire[22] in 1947 at a frequency of 15 MHz. Several other experiments were performed to increase the temperature and frequency range and to determine the absorption and the velocity of sound more accurately. In 1958, Chase[23] realized for the first time that the maximum in attenuation occurred below the transition but, since these measurements were conducted in an open bath, the submillidegree resolution which would have been necessary to assert this fact could not be reached. Higher temperature resolution techniques were used by Barmatz and Rudnick,[24] who were able to pinpoint the temperature of the shifted maximum and more recently, Williams

and Rudnick[25] evaluated quantitatively the temperature of the peak for frequencies between 600 KHz and 3 MHz.

At higher frequencies, the work of Imai and Rudnick[26] at 1 GHz showed a very sharp peak in the region of the transition and indicated that the maximum occurred at 3×10^{-3} °K below T_λ . This result was somehow uncertain for the same reasons invoked above in the case of Chase's experiment. The purpose of the present investigation was to develop a technique to determine with a high temperature resolution the behavior of the attenuation in the vicinity of T_λ and the position of the maximum. Other high frequency measurements have been performed[27-29] using the Brillouin scattering technique, but no conclusion can be reached regarding the temperature of the attenuation peak.

An important aspect of measurements such as those reported here lies in the fact that the phenomena observed in liquid helium might be generalized to other order-disorder transitions. In fact the similarity between the behavior of first sound near the lambda point of liquid helium and near the critical temperature of another substance has already been observed[30]; in nickel the attenuation maximum is located below the magnetic critical point and is temperature dependent.

II. ATTENUATION OF FIRST SOUND NEAR T_λ, THEORY

Many theories have attempted to explain the anomalous attenuation of first sound in the vicinity of a phase transition or critical point. In spite of the fact that experiments have shown for some time that there exists a shift of the attenuation maximum, no attempt has been made so far to devise a unified theory which would predict the experimental observations. Also, most of the existing theories are restricted to low frequencies such that the product $\omega\tau << 1$, where τ is a relaxation time. Therefore, it is not clear whether any of the existing theories can be used to explain the measurements performed at high frequencies.

At a given temperature, the total attenuation is due to several causes, besides the well known losses due to the shear viscosity and thermal conductivity.

A recent study of ultrasonic propagation at low frequencies in liquid helium near the lambda point[25] has been interpreted by such a combination of attenuation processes; the attenuation maximum could be attributed to a) a symmetric attenuation maximum due to fluctuations of the order parameter and b) a relaxation peak which is present only below the lambda transition. A similar interpretation will be attempted here and a brief account will be given of the absorptions due to fluctuations and to relaxation processes.

2.1 Attenuation Due to Fluctuations

Spontaneous internal fluctuations of a system in thermal equilibrium in the vicinity of a phase transition, or critical point, can be a cause

for the anomalous attenuation of ultrasonic waves. The first sound waves interact with the fluctuations and give rise to an absorption which is symmetrical with respect to the lambda point, since fluctuations occur below and above the transition. The magnitude of the effect depends on the coupling of the sound wave, that is, of the pressure or density, to the mean square value of the order-parameter. This mechanism was first studied by Ginzburg.[31] Levanyuk,[32] using a time-dependent Ginzburg-Landau theory of second order phase transitions, performed the first detailed calculation of the interaction between a sound wave and intrinsic time-dependent fluctuations. The results show that an increase in the fluctuations of the characteristic transition parameter is responsible for an increase in the attenuation both above and below the transition. However, the temperature and frequency dependences do not match all the experimental data. Stauffer and Wong[33] reconciled the classical time dependent Landau[16] theory of second order phase transitions and the scaling laws[17,18,34]; they conclude that parafluidity, i.e., the enhancement of fluidity due to order-parameter fluctuations, is manifested in the divergence of the first sound attenuation, which is found to vary as ε^{-1} above T_λ if a relaxation time τ_o proportional to ε^{-1} is used. Below T_λ, they conclude that the main contribution of the attenuation is a Landau-Khalatnikov relaxation peak, which will be explained in the next section.

Wong[35] studied the hypersonic attenuation and derived from a theory of relaxation of the order parameter in the critical regime ($k\xi >> 1$) that the attenuation has a broad symmetric maximum centered at T_λ. Its temperature dependence is asymmetric: ε^{-1} for $T < T_\lambda$ and

$\varepsilon^{-1/2}$ for $T > T_\lambda$; and its frequency dependence is ω^2 both below and above the transition. In a supercritical region for which nonlinear fluctuations become important and which is estimated to have its threshold at a frequency of 10 GHz the attenuation should be symmetrical. It was not possible to determine whether the experimental data of Imai and Rudnick[26] obtained at 1 GHz were exhibiting this supercritical phenomenon.

Kawasaki[36,37] has investigated high-frequency first sound attenuation using the mode-mode coupling theory and the static and dynamic scaling theories. The region of frequencies where this theory is valid has the characteristic frequency of order-parameter dynamics as a lower limit. The higher limit is the frequency of a sound wave whose wavelength is equal to the correlation range of local order-parameter fluctuations. When the frequency ω is larger than the average relaxation frequency $\tau^{-1} = u_2/\xi$ where u_2 is the velocity of second sound and ξ the correlation length, the various wavevectors k characteristic of the spontaneous fluctuations correspond to frequencies larger and smaller than ω; only those which have a relaxation time smaller than ω^{-1} will contribute to the attenuation. This corresponds to an effective cutoff relaxation time τ_{eff} which is frequency dependent. The attenuation can be written

$$\alpha(\omega) = \frac{\Delta u}{u_0^2} \left[\frac{\omega^2 \tau_{eff}}{1 + \omega^2 \tau_{eff}^2} \right] \qquad (13)$$

Assuming a linear dependence $\tau_{eff} \propto \omega$ for $\omega\tau >> 1$

$$\alpha(\omega) = \frac{\Delta u}{u_0^2}\, \omega \qquad (14)$$

$\Delta u = u_\infty - u_o$ is the difference between the high frequency and low frequency limits of the first sound velocity. The interesting consequence of this theory is that

$$\alpha' \propto \omega \varepsilon^{\circ} \qquad \omega\tau \gg 1 \tag{15}$$

This attenuation maximum is roughly symmetric about the transition.

A recent calculation of high frequency hydrodynamics[38] confirmed this result.

2.2 Attenuation Due to Relaxation Processes

Considering the relaxation mechanism associated with the order-parameter, Landau and Khalatnikov[39] were able to predict the presence of an attenuation peak in the vicinity of a second-order phase transition. Since they used the Landau[16] theory of second order phase transitions which does not apply to the lambda transition of liquid helium, the same results were rederived by Pokrovskii and Khalatnikov[40] using the modified hydrodynamic equations of Pitaevskii. The superfluid density ρ_s plays the role of the independent variable instead of the order parameter. The time characteristic of the relaxation of the superfluid density when it is disturbed from equilibrium is

$$\tau = \frac{\xi}{u_2} \tag{16}$$

where ξ is the order parameter correlation length and u_2 is the velocity of second sound.

The relaxation time of the normal density is shorter; τ_1 is ν_A^{-1} where ν_A^{-1} is the interatomic collision time. For low frequency sound waves, this relaxation process may be considered instantaneous; for the

high frequency waves used in this experiment, τ_1 might scale as ω^{-1}. It must be noted, however, that the Pokrovskii-Khalatnikov theory is valid only for low frequencies, and its range of validity should be extended to cover the present results.

The absorption of acoustic energy is attributed to the generation of second sound by the first sound waves. The first sound attenuation associated to a relaxation process[41] can be written

$$\alpha(\omega) = \frac{\Delta u}{u_s^2} \frac{\omega^2 \tau}{1 + \omega^2 \tau^2} \tag{17}$$

It is maximum at

$$\omega \tau = 1 \tag{18}$$

Since the correlation length ξ is inversely proportional to the superfluid density ρ_s and since the velocity of second sound u_2 goes as the square root of ρ_s,

$$\xi \propto \rho_s^{-1} \quad , \quad u_2 \propto \rho_s^{1/2} \tag{19}$$

$$\tau = \frac{\xi}{u_2} \propto \frac{\rho_s^{-1}}{\rho_s^{1/2}} \propto \rho_s^{-3/2} \tag{20}$$

Since $\rho_s \propto \varepsilon^{2/3}$, then $\tau \propto \varepsilon^{-1}$. The maximum in attenuation therefore occurs at $\omega\varepsilon^{-1}$ = constant. This determines the temperature of the attenuation maximum for a given frequency. Except for the fact that it is a simple assumption, there exists no theoretical justification for the presence of a single relaxation time. In a detailed microscopic analysis, Pokyakov[51] showed that the collective excitation spectrum is defined by several scaling lengths. He concluded that the anomalous

attenuation of sound is induced by two mechanisms: a one-particle relaxation mode and a thermal relaxation mode. This implies that at least two correlation lengths, or two relaxation times, play a role in the absorption mechanisms of sound waves in the vicinity of an order-disorder transition.

III. EXPERIMENTAL APPARATUS

In its first stage, this experiment consisted in carefully reproducing the data obtained by Imai,[42,26] using the variable path interferometer that he described. The system, schematically shown in Fig. 8, consists of a pulsed oscillator which feeds two signal paths: the acoustical path yielding a signal of amplitude V_A, which can be varied by adjusting the distance between the transducers, and an electrical path yielding a signal amplitude V_E. The sum of these signals, depending on their relative phase, has a value which lies between a maximum $|V_A+V_E|$ and a minimum $|V_A-V_E|$ as shown in Fig. 9. As the acoustical path is increased, the amplitude oscillates between these limits over an acoustic wavelength, and the exponential decrease of V_A is reflected by the exponentially decreasing envelope as shown in Fig. 10. This method leads to an absolute value of the attenuation.

In its second stage, a sealed interferometric system was conceived. It is isolated from the helium bath by a vacuum jacket to permit control of its temperature within a fraction of a millidegree. Since the acoustical path is fixed, it gives a relative measurement of the attenuation. This system will be described here in detail.

3.1 Cryogenic System

The low temperatures needed to conduct this experiment were obtained in a standard silvered glass double dewar system (Fig. 11). The inner dewar had a working inner diameter of three inches and held about five liters of liquid helium. The outer dewar was filled with liquid nitrogen to precool the cryostat and the acoustic probe. The two dewars were

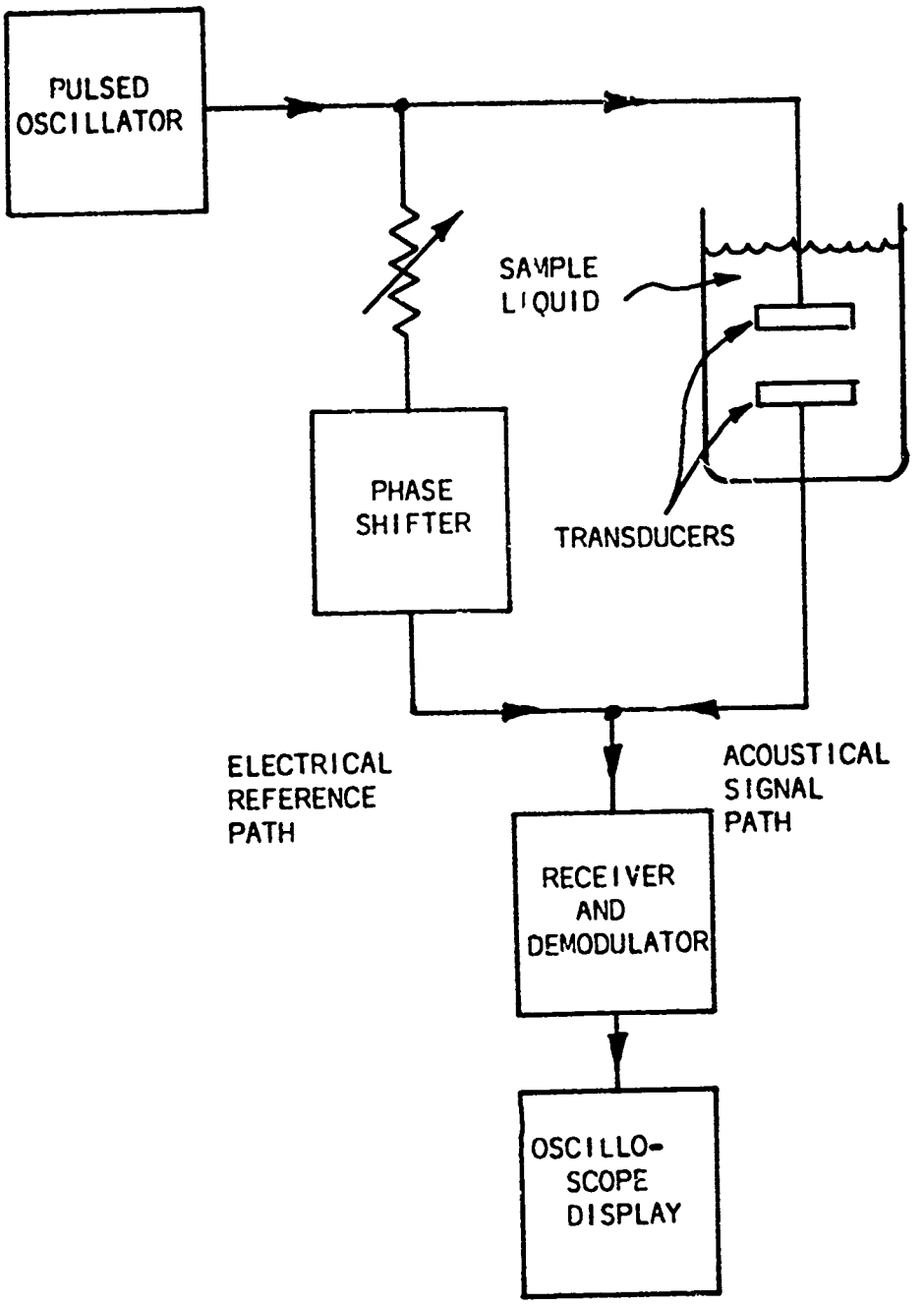

FIGURE 8.

SIMPLIFIED BLOCK DIAGRAM OF THE INTERFEROMETER SYSTEM

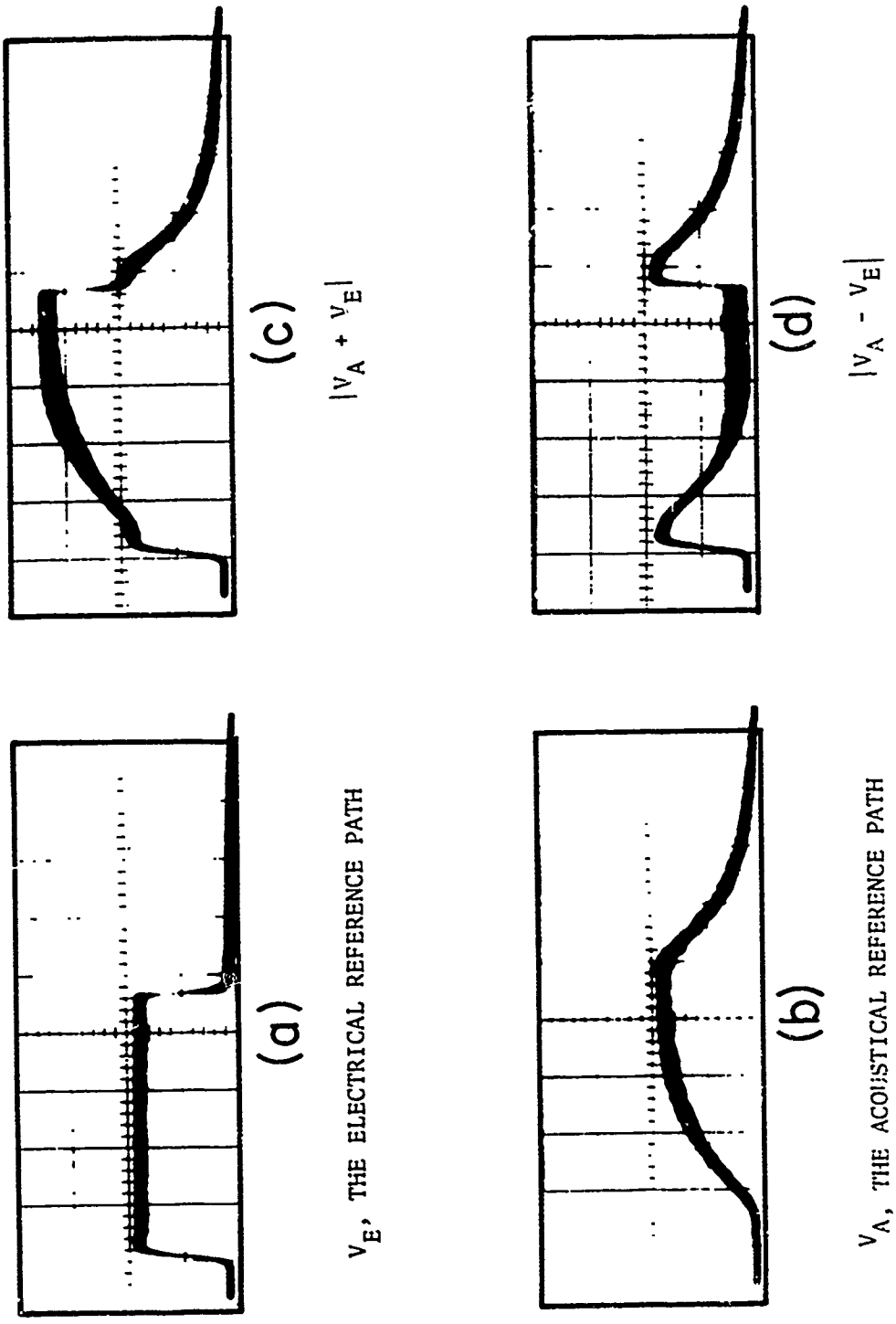

FIGURE 9.

THE DEMODULATED RECEIVED SIGNAL UNDER A VARIETY OF CONDITIONS
THE PULSE LENGTH IS APPROXIMATELY 40 MICROSECONDS

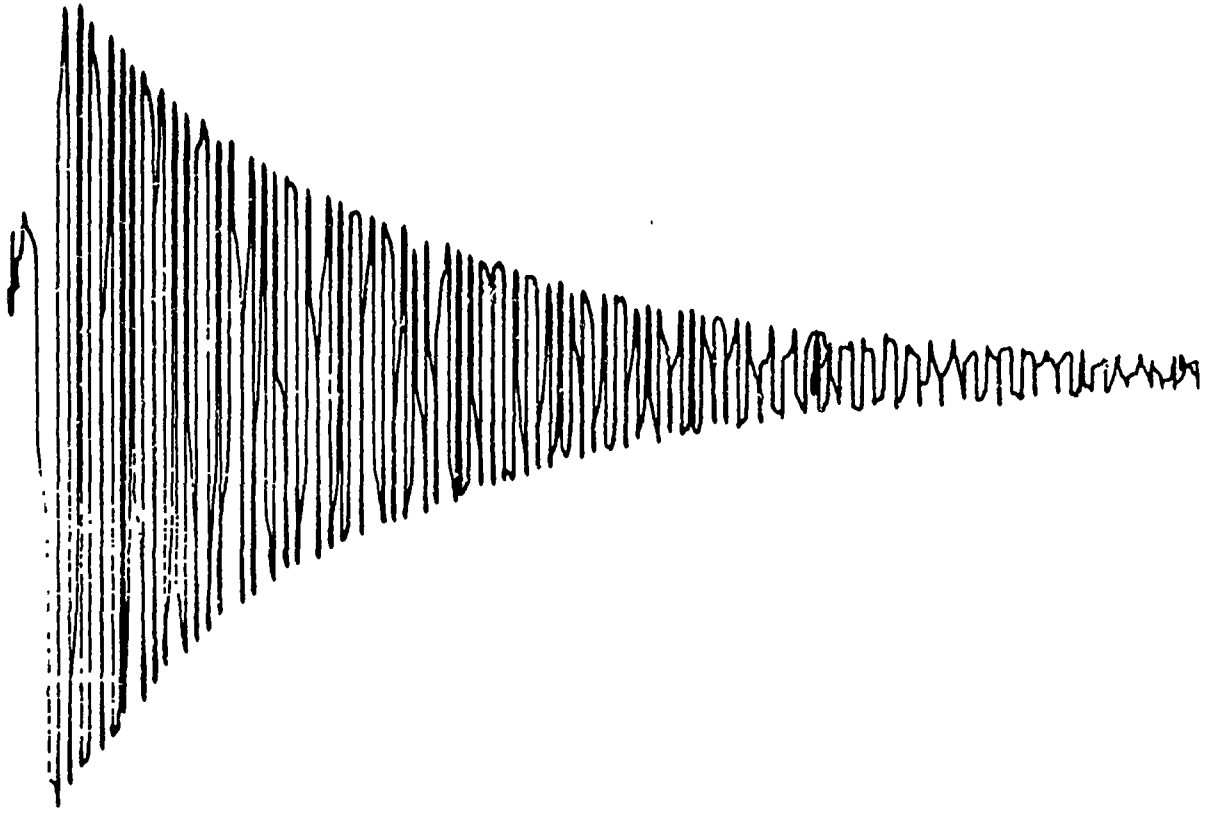

FIGURE 10.
RECEIVED SIGNAL AMPLITUDE vs. DISTANCE

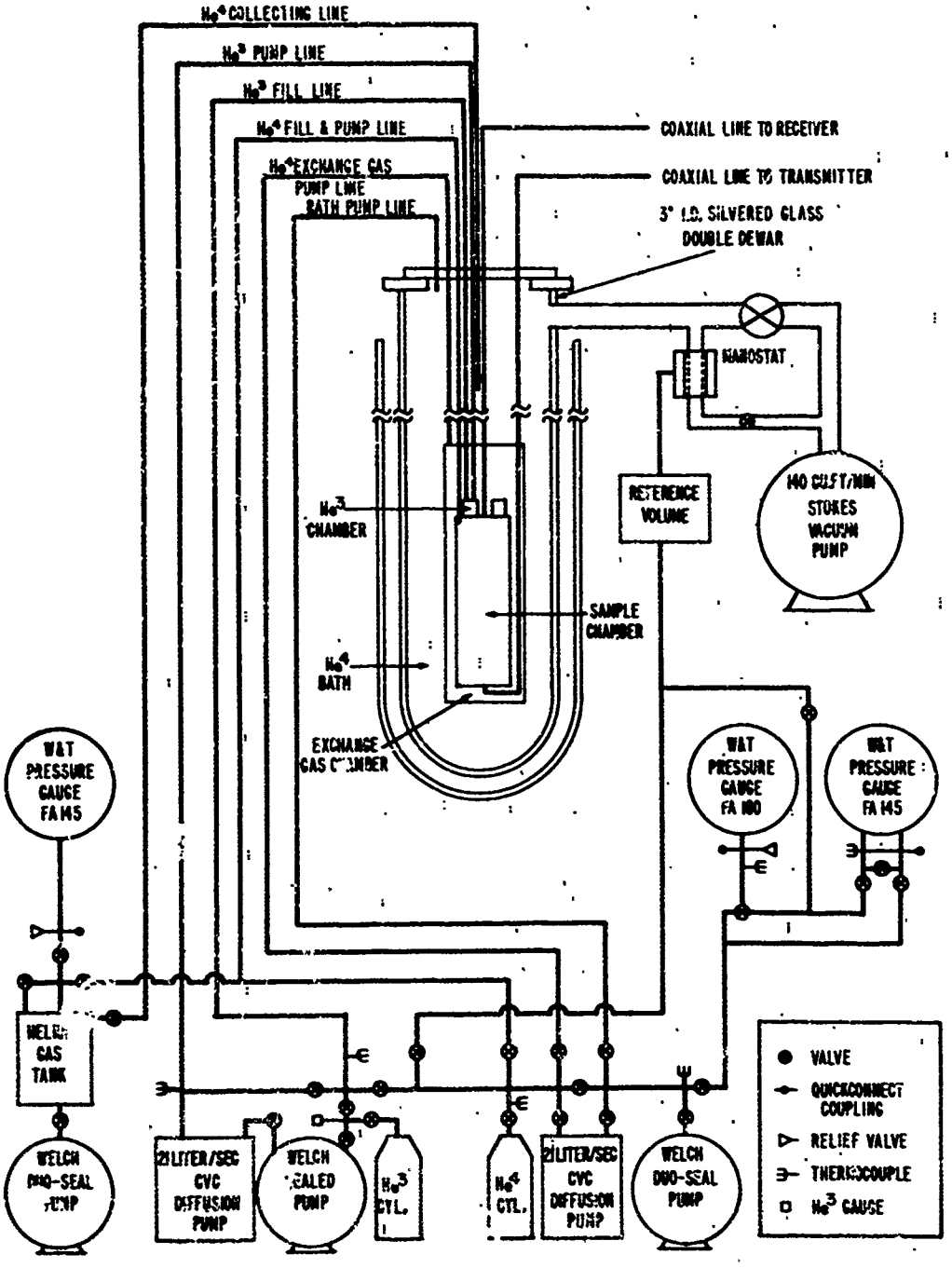

FIGURE 11.

CRYOGENIC SYSTEM

isolated from each other by a vacuum jacket which, during the precooling phase, was filled with about 1 mm of nitrogen gas.

The temperature of the liquid helium was lowered by pumping the helium vapor by means of a 140 cu-ft/min pump (Stokes Model 212); temperatures as low as 1°K could be obtained. The temperature of the helium bath was controlled by the manostat described by Imai[42] and could be regulated to within $\pm$ 0.001°K. The bath temperature was monitored by two dial manometers (Wallace and Tiernan models FA-160 and FA-145) and, when necessary, by a Texas Instrument model 145 precision pressure gauge.

A helium gas reference tank was available, so that it was possible to collect helium gas of extremely high purity directly from the helium bath and to condense it later in the sample chamber. A dial manometer (Wallace and Tiernan FA-145) could be used to monitor the pressure of the helium gas tank and therefore determine the amount of gas condensed in the sample chamber.

The system was also equipped with a He^3 refrigerator[43] consisting of a He^3 tank, a sealed pump (Welch 5 cu-ft/min) and a diffusion pump (CVC 21 liter/sec). He^3 gas could be condensed in the He^3 chamber of the experimental probe and by isolating the probe from the He^4 bath and pumping on the He^3 chamber, temperatures below 1°K could be reached, if needed.

The liquid air level in the outer jacket was maintained above a preset level by a level controller consisting of a thermistor activating a Schmidt trigger.[44] A timer, in series with the level controller, protected the installation against a prolonged malfunction.

3.2 Acoustic Probe and Transducers

The acoustic probe is shown on Fig. 12. It consists of three independent chambers: the sample chamber, which holds the two cadmium sulphide transducers and several temperature sensors; the He^3 chamber where He^3 gas can be condensed and evaporated to cool the sample below 1°K; and an exchange gas chamber, used to isolate the sample chamber from the helium bath or, during the cooling phase, to put the sample chamber in intimate thermal contact with the bath.

3.2.1 Sample Chamber

The sample chamber (Figs. 13, 14) was a cylindrical cavity 2" long and about 4/3" I.D. It was supported by the 1/4" thin walled He^3 line. To minimize the heat leak between the helium bath and the sample chamber, this tube was made out of stainless steel which at helium temperatures has a small heat conductivity. The He^4 gas was fed to the sample chamber, after having been collected from the bath, through a 0.025" O.D. stainless steel tube. This capillary was terminated by a flange which was screwed to the sample chamber and sealed by a 0.026" diameter indium "O" ring. A 1500 ohm heater was wound into a groove around the chamber using Manganin resistive wire (30.7 Ω/ft) and was covered with GLYPTAL. Six electrical feedthroughs were built into the wall of the chamber so that several thermometers could be installed in the sample: they were composed of a copper core, which was epoxied to the wall (Stycast 2850 GT and Catalyst 24 LV); two monel prongs were soldered to the core of each feedthrough, so that the connecting wires could be soldered and unsoldered without overheating the epoxy.

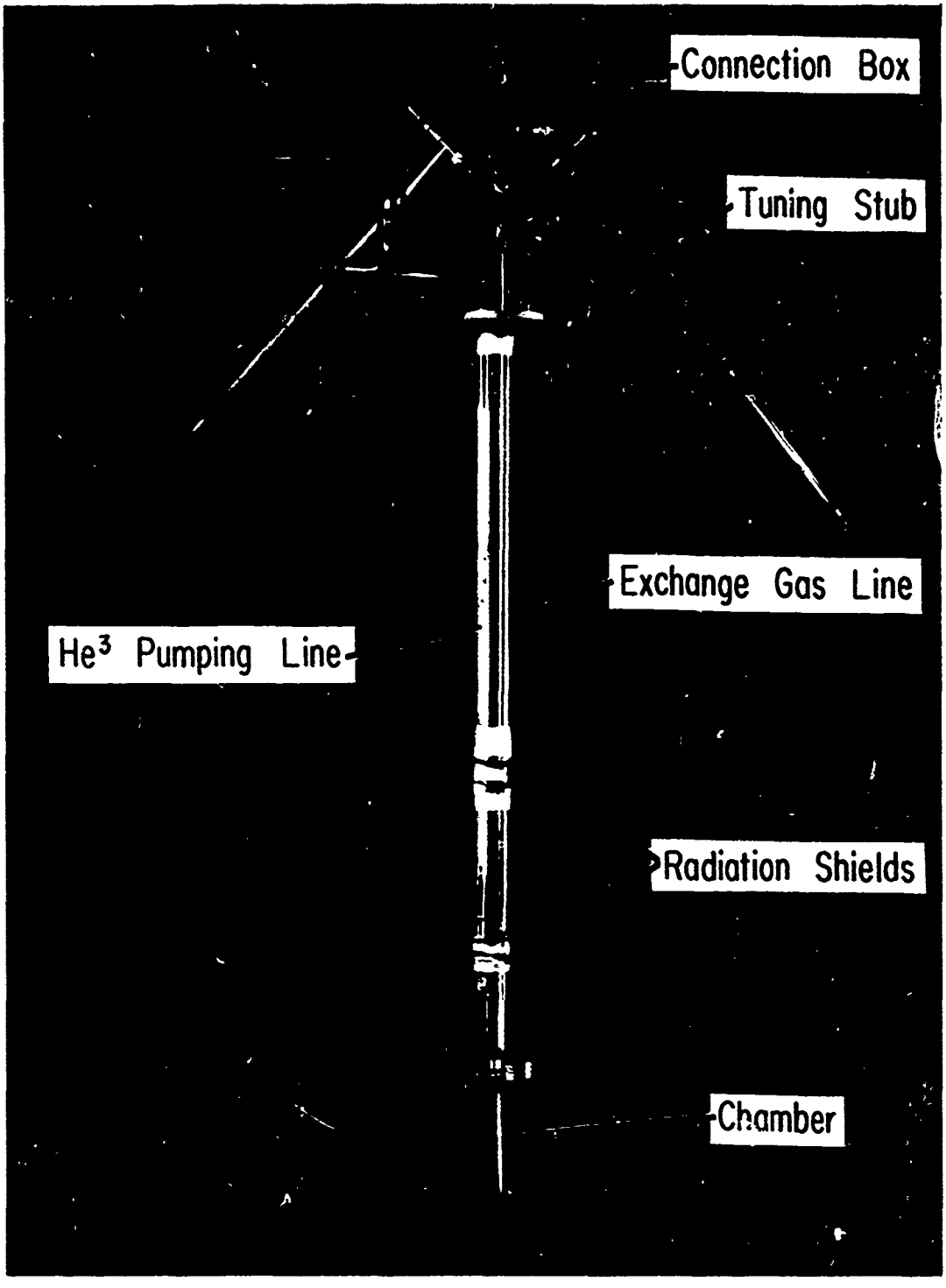

FIGURE 12.

ACOUSTIC PROBE

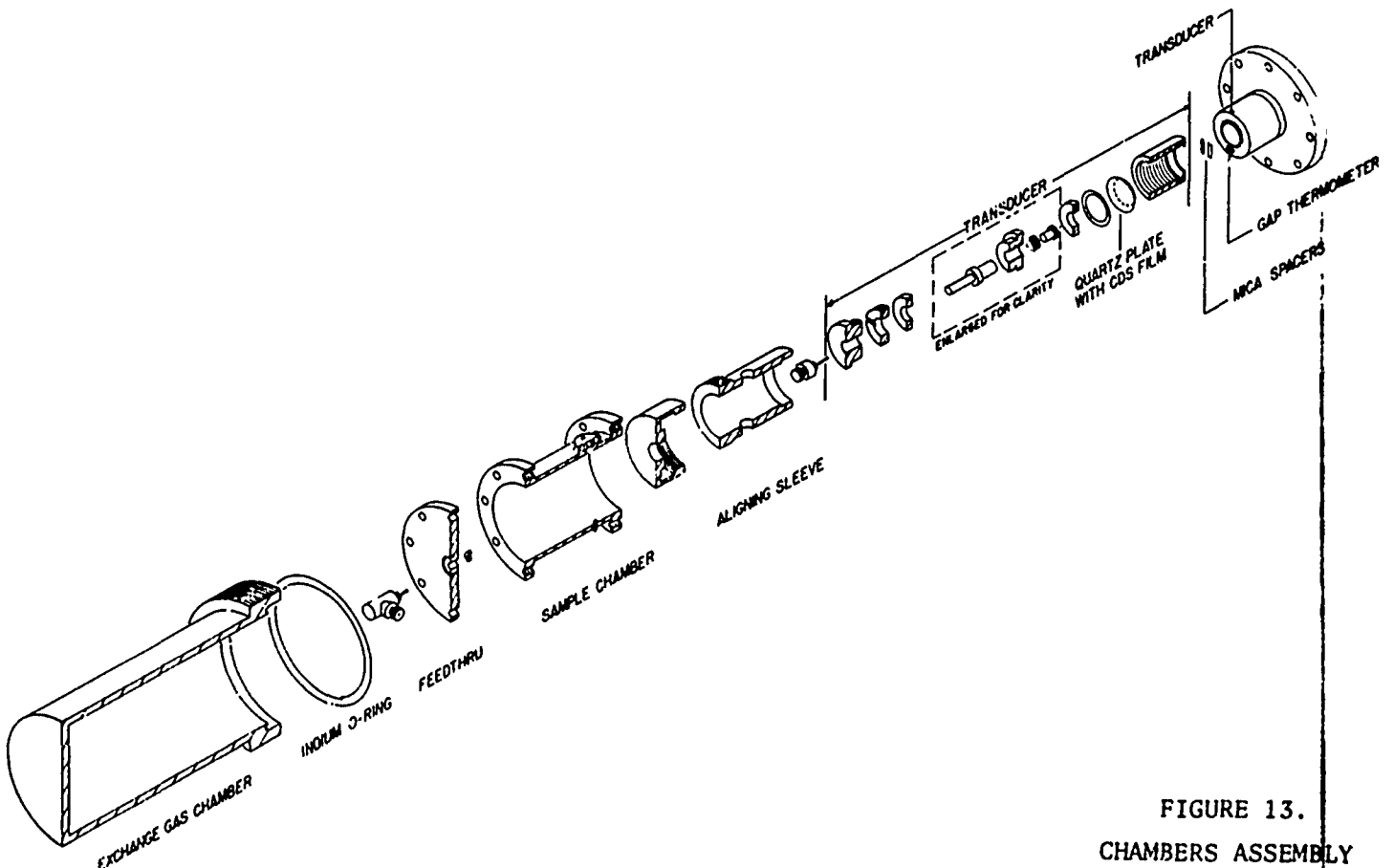

FIGURE 13.
CHAMBERS ASSEMBLY

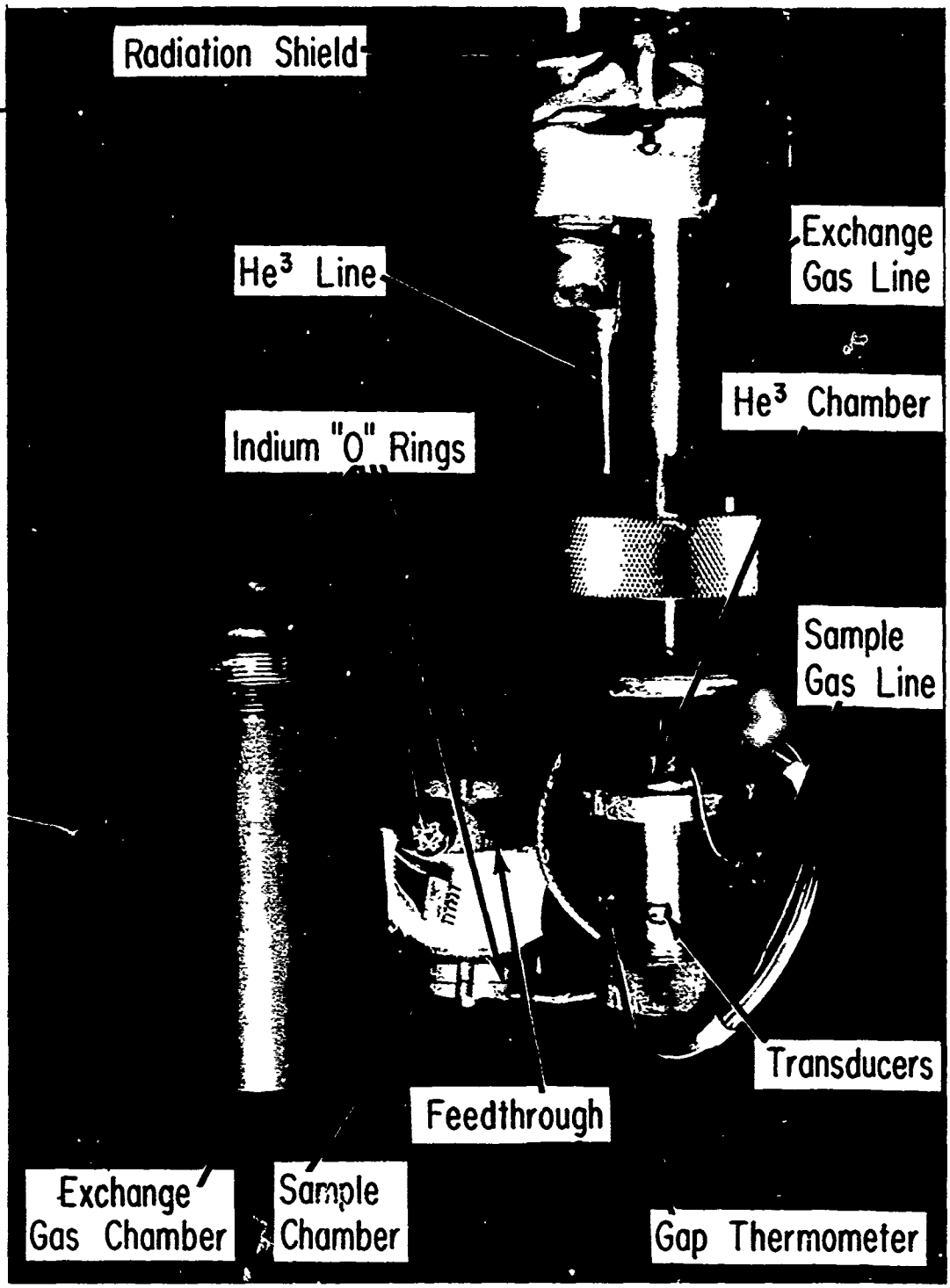

FIGURE 14.

SAMPLE CHAMBER

The bottom flange was sealed to the body of the chamber by a 0.032" indium "O" ring and served as a coaxial connector to the bottom transducer; for this purpose a MICRODOT 051-0315 plug was soldered in its center. The top flange was similarly used as a seal and as a connector, since it had an indium "O" ring and a MICRODOT 051-0049 connector but it was also the reservoir of the helium-three evaporative cooling system. The reservoir was given an annular shape so that the center of the plate was made available for the coaxial connector. The purpose of the grooves was to provide an intimate thermal contact between the helium-three condensate and the sample chamber.

The sample chamber was contained in the exchange gas chamber and all the leads and coaxial lines were pinned thermally to the helium bath since they were soft-soldered or epoxied (STYCAST 2850 GT) to the copper flange of the exchange gas chamber.

3.2.2 Connection Box

The connection box (Fig. 15), at the top of the probe, was given a cylindrical shape and its axis was horizontal. The front flange could be screwed onto the body of the box and a rubber "O" ring was used to seal the system. Two connectors (AMPHENOL type N) were provided and connected to the transducers by coaxial cables (MICROCOAX UT-141-SS) which introduced an attenuation of 25 db/100 ft. Two tuning stubs (MICROLAB SL-03 N) could be mounted directly on the connectors. The various electrical leads were connected to a multi-prong glass-to-metal feedthrough. A 1/2" "Quikonnect" (from Goddard Valve Corp.) was connected to the He^4 exchange gas pump line. Three 1/4" Quikonnect fittings were installed

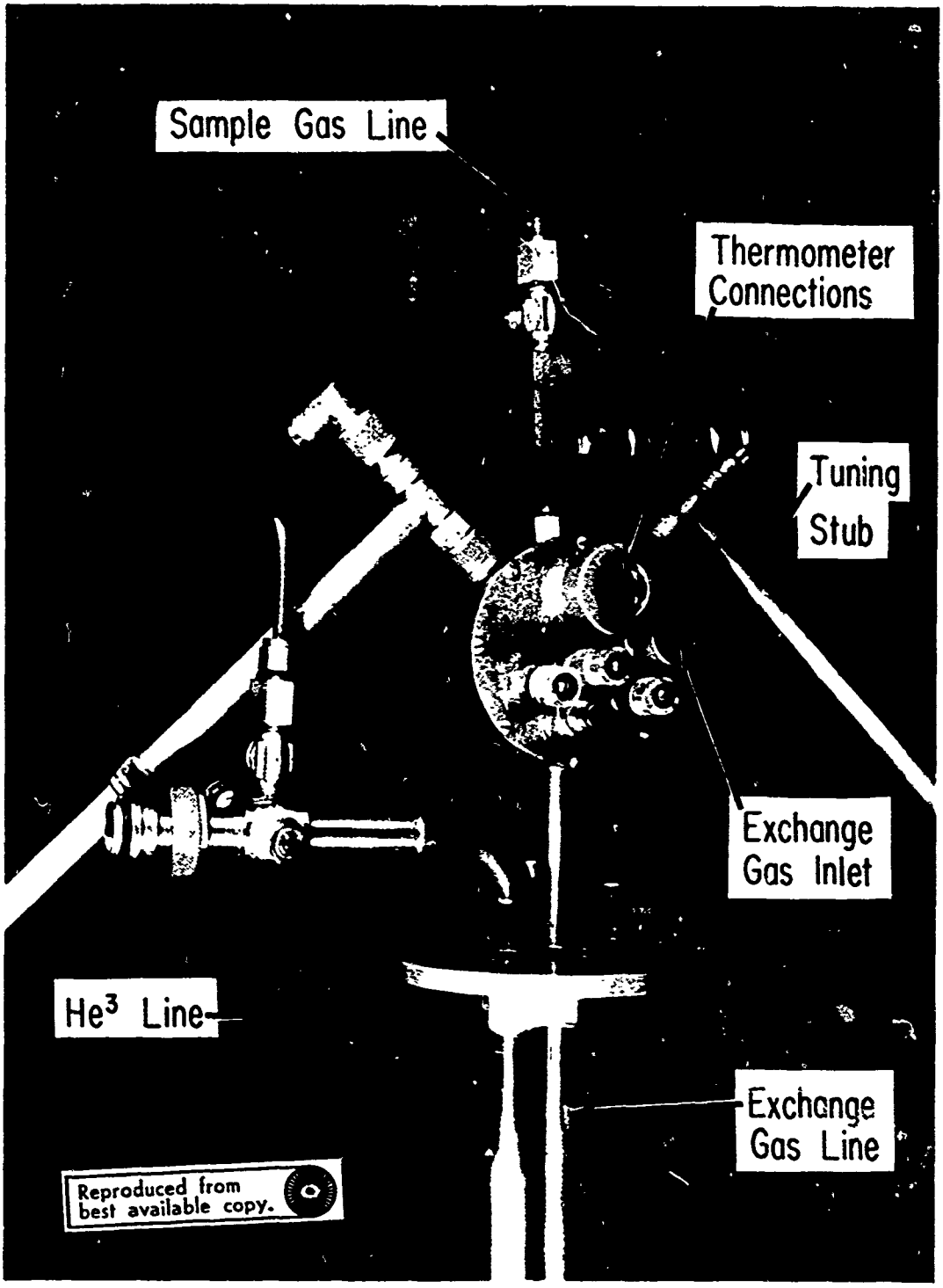

FIGURE 15.

CONNECTION BOX

so that a mechanical system could be used if necessary. A relief valve was also mounted on the box for safety purposes.

The filling line of the sample chamber went clear through the top of the connection box and was linked to the cryogenic system through a needle valve. A relief valve, a thermocouple gauge, and a discharge vacuum gauge were provided.

3.2.3 Transducers

The purpose of this investigation was to study the propagation of sound waves at a frequency of 1 GHz. The transducers used were [illegible] sulphide films deposited on quartz substrates.

Cadmium sulphide[45] crystallizes in a hexagonal wurtzite structure and is one of the simplest crystals lacking a center of symmetry and, therefore, exhibiting pieozoelectricity. Its electro-mechanical coupling constants are considerably greater than those for quartz.[46]

Moreover, such transducers are unaffected by thermal shock and magnetic field and can be used at their fundamental resonant frequency or at an odd harmonic in the gigacycle range.

The quartz substrates were 12 mm in diameter and 2 mm thick, optically flat to 1/20 wave of green light and parallel to 3 sec of arc. The edges were beveled at 45° angle. A rather complicated, but mandatory, cleaning procedure was used; the films have a tendency not to adhere to the substrates if they are not perfectly clean. Moreover, epitaxial growth might not occur. The plates were washed first in concentrated nitric acid, then in concentrated sodium hydroxide. They were then rinsed in distilled water and boiled for several minutes in ethyl

alcohol. The ethyl alcohol vapor was then used to dry the samples. They were immediately transferred to a vacuum chamber and submitted to an intense ion bombardment (700 V to 1000 A.C. volts under 100 to 200 microns pressure) for 10 to 20 minutes. A coating of gold, with an underlay of chrome for adhesion, was vacuum evaporated on one side of the sample. Since both sides of the quartz plate had to be coated with gold to minimize the radio-frequency cross-talk between the transducers, the vacuum was briefly broken and the plates turned over; then the coating process was repeated. The plates were cooled and kept under a pressure of 10^{-6} to 10^{-7} mm Hg.

The cadmium sulphide must be evaporated onto the back of the quartz substrate with its c-axis normal to the substrate in order to generate efficiently longitudinal waves. A rotation of the c-axis leads to the unwanted generation of shear waves in the substrate, thereby decreasing the efficiency of the system.

The simplest evaporation technique,[42,47] making use of CdS powder only, does not always result in a good stochiometry because the partial pressure of the sulphur is too low. This situation can be remedied by simultaneously vaporizing CdS and S or, better, Cd and S in two independently monitored crucibles.[48]

A schematic diagram of the vapor-deposition chamber is given in Fig. 16. To increase the probability of obtaining an identical pair of transducers, the piezoelectric substance was deposited in one operation on two quartz plates. The substrates could be heated and held at a temperature T such that 180°C < T < 200°C. This temperature range was chosen to insure that neither pure cadmium nor pure sulphur would deposit

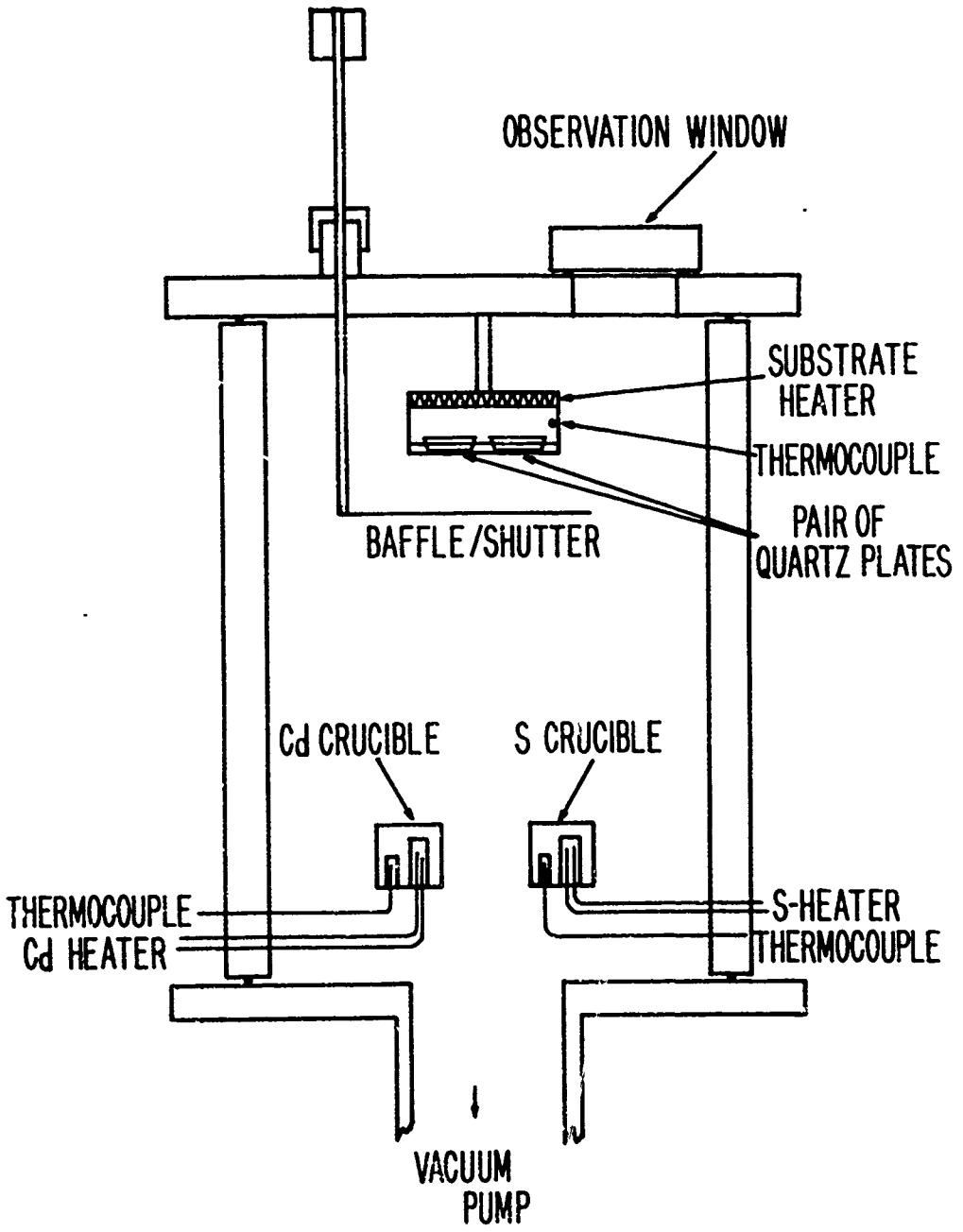

FIGURE 16.

CADMIUM SULPHIDE VAPOR-DEPOSITION CHAMBER

from the vapor. Two separate crucibles were used, one for cadmium and the other for sulphur. Each crucible had its own heater and thermocouple.

During the preheating phase, necessary to bring the cadmium and sulphur to their boiling point and to adjust the vapor emission, a shutter was placed directly below the substrates to isolate them from the vapor. During the actual deposition, the shutter could be either completely removed or simply lowered to play the role of a baffle. Though the two methods gave positive results, the second was used since it gave more reproducible films. Without a baffle the operation lasted only a few minutes. The baffle, which protected the substrate from the direct molecular beams, slowed down the deposition rate and one or two hours were necessary to obtain the expected result. The deposition rate on the observation window gave an excellent idea of the amount of CdS deposited on the quartz.

At the end of the operation the shutter was used to stop the deposition.

The transducers were then mounted in holders made out of gold-plated brass and teflon (Fig. 17). Only a small central region with a diameter of 1 mm was excited to help reduce the critical alignment problem.

The transducers could then be mounted in the sample chamber. An aligning sleeve made sure that they were centered properly.

Since it was known from previous results[26] that the attenuation could be of the order of 2500 cm^{-1} near the lambda point and therefore that the amplitude of the emitted sound wave could be reduced to 1/e of its value over approximately 40,000 Å or 20 wavelengths, the distance

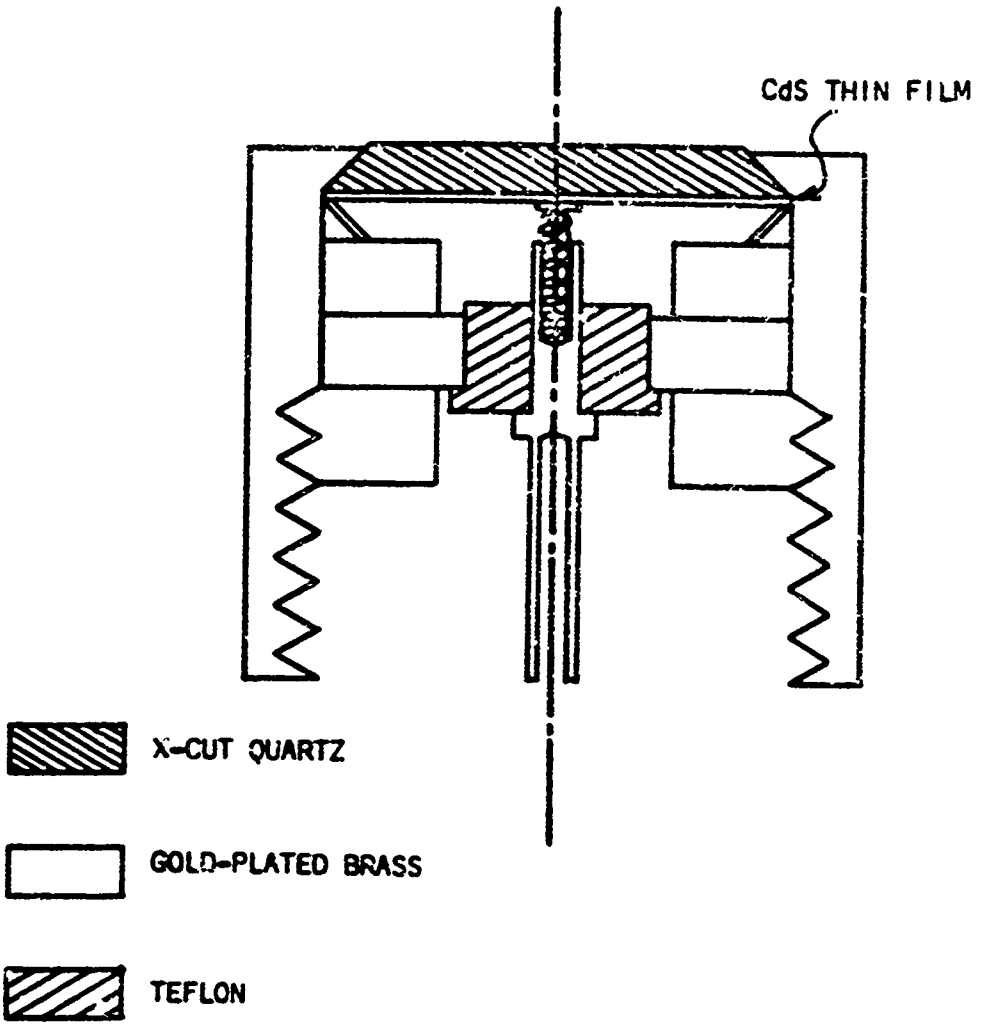

FIGURE 17.

TRANSDUCER ASSEMBLY

between the transducers was set at about 2×10^5 Å or 100 wavelengths. Two narrow strips were cut from a mica sheet 0.7 to 0.8 mils thick and were pressed between the two quartz plates. The separation between the mica strips was approximately 5 mm. The spacers also made sure that the quartz plates were sufficiently parallel. Since the active portion of the transducers was 1 mm in diameter, phase cancellation occurred if the non-parallelism exceeded or equaled an angle of 10^{-4} radians.

IV. MEASUREMENT TECHNIQUES

4.1 Transfer Procedures

The dewar and the acoustic probe were cooled down to about 77°K and maintained at that temperature by keeping the liquid nitrogen jacket of the double dewar full and filling the vacuum jacket with about 1 mm of nitrogen gas.

Liquid helium was transferred into the dewar and helium gas was collected directly from the vapor of the bath and stored in the helium gas tank at room temperature. This 20 liter volume was filled to one atmosphere and sealed off.

A small amount of helium gas, 20 μ Hg, was introduced in the exchange gas chamber and in the sample chamber to put them in good thermal contact with the helium bath, which could then be cooled to approximately 1.5°K by pumping on its vapor.

Through a needle valve, helium gas was slowly transferred from the helium gas reference tank in the sample chamber. The warm helium gas heated the sample chamber and the condensation rate was adjusted so that the chamber was always kept under the lambda temperature. The mass of gas transferred could be determined by monitoring the initial and final pressures of the helium gas tank. It was also possible to know that the chamber had been filled above the transducer level by observing the transmission of sound through the sample.

The chamber was then sealed off and was ready for the experiment. To keep the system operational for a long period of time, one half-day or more, it was only necessary to replenish the supply of liquid helium

in the inner dewar.

4.2 Temperature Measurements

The sample chamber contained two thermometers: one was an Allen-Bradley 1/10W, 82 Ω carbon resistor and the other was a Cryoresistor, CR 50-VC from Cryocal, Inc., which could be used for measurements below 1°K. The carbon resistor was placed at the level of the gap and as close as possible to the acoustic field, namely 7 mm from the center of the transducers.

The change in resistance was measured on a Wheatstone bridge of high precision (Fig. 18) and the deviation from equilibrium could be measured on a D.C. null voltmeter. A direct recording of this deviation could be obtained simultaneously with a recording of the amplitude of the acoustic signal. The power dissipated in the resistor was limited to a few microwatts to prevent self-heating effects from disturbing the measurements.

To calibrate the resistor, helium gas was condensed in the exchange gas chamber and all the chambers were connected through the external lines. The pressure above the helium bath was measured by a Wallace and Tiernan model FA 160 absolute pressure gauge and a high precision Texas Instrument Model 145 pressure gauge. At each point, the system was given several minutes to reach equilibrium and the value of the resistor was read only when the stability was satisfactory. For comparison purposes, another Allen-Bradley 1/10 W, 82 Ω carbon resistor was hung in the helium bath and measured at each point. It should be noted that, even though the sample chamber was thermally in contact with the helium

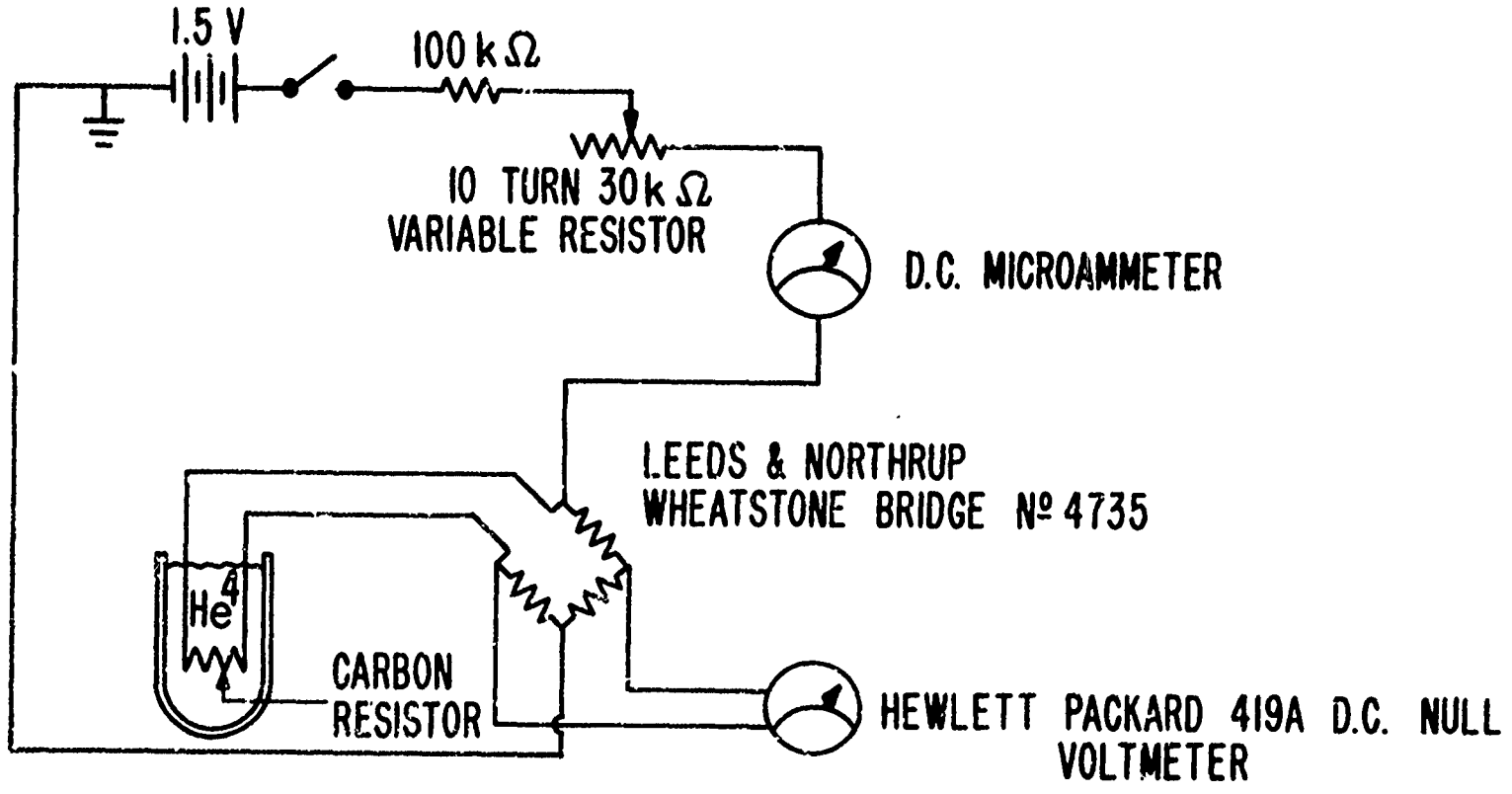

FIGURE 18.

SCHEMATIC OF CARBON THERMOMETER NETWORK

bath, the stability of the liquid contained in the sample chamber was much greater than that of the bath.

The location of the lambda point was determined by the characteristic step in resistance due to the change in self-heating as the lambda point is crossed.

4.3 Attenuation Measurements

4.3.1 Electronics

Each transducer was tested individually using the circuit shown in Fig. 19. The best self-resonance frequency of the transducer was found by varying the frequencies of both the pulsed oscillator and the local oscillator. The intermediate frequency was 30 MHz. The tuning stub was adjusted so that a maximum power would be delivered to the load and the strongest self-resonance could be observed. A typical result is shown in Fig. 20. It should be pointed out that the performance of the transducers was greater at helium temperature than at room temperature since the internal losses in the quartz are less in a cold system.

Each transducer and stub combination had to be individually adjusted at the same frequency, in order to obtain a matched pair, which is a mandatory requirement if the transducers are operated at resonance.

To measure the attenuation, the configuration of Fig. 21 was used. As explained in Chapter II, if this circuit was used with the variable path interferometer, the absolute attenuation could be measured at a given temperature. The gate width and delay could be set to sample the portion of the signal in the shaded area of Fig. 22. By varying the spacing between the transducers, the amplitude oscillated between $|V_A+V_E|$

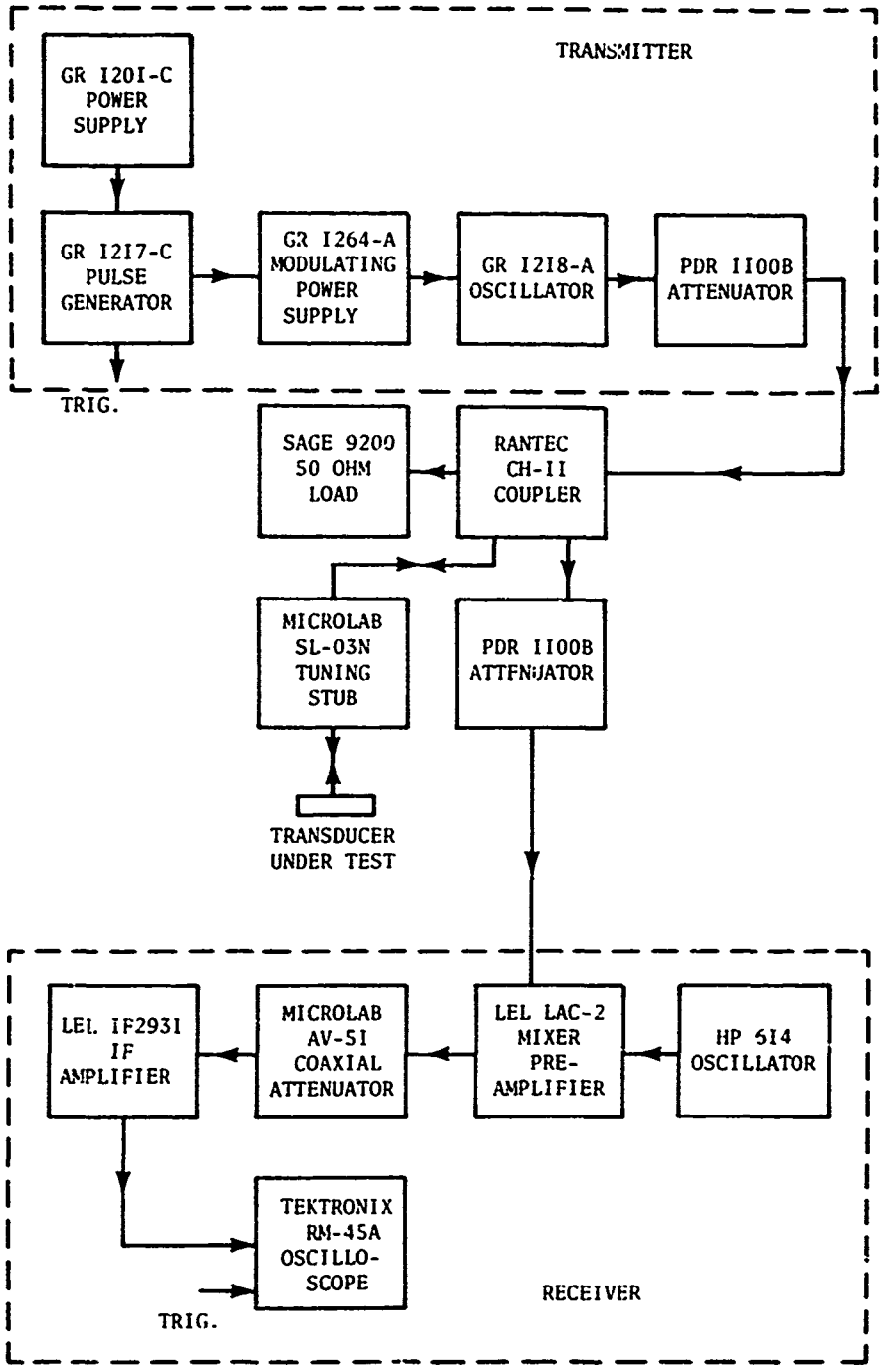

FIGURE 19.

BLOCK-DIAGRAM FOR TESTING RESONANCE OF INDIVIDUAL TRANSDUCERS

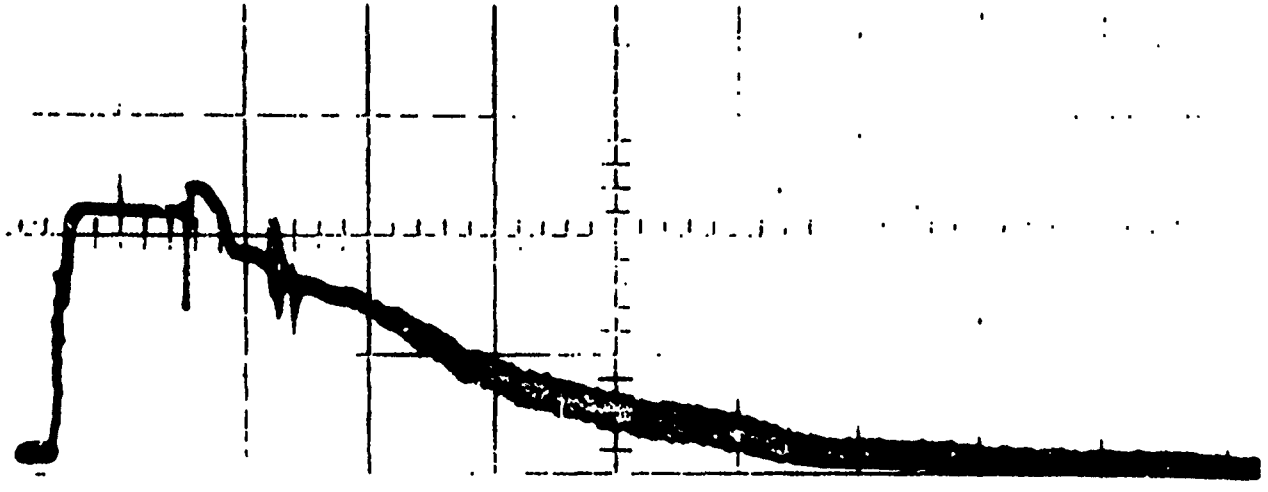

FIGURE 20.

OSCILLOSCOPE DISPLAY ILLUSTRATING RESONANT RESPONSE OF AN INDIVIDUAL TRANSDUCER.THE TRAILING SIGNAL IS DUE TO RINGING AND INDICATES EXCITATION AT A CHARACTERISTIC MODE. THE RINGING MAY PERSIST FOR AS LONG AS 100 MICROSECONDS AT HELIUM TEMPERATURES.

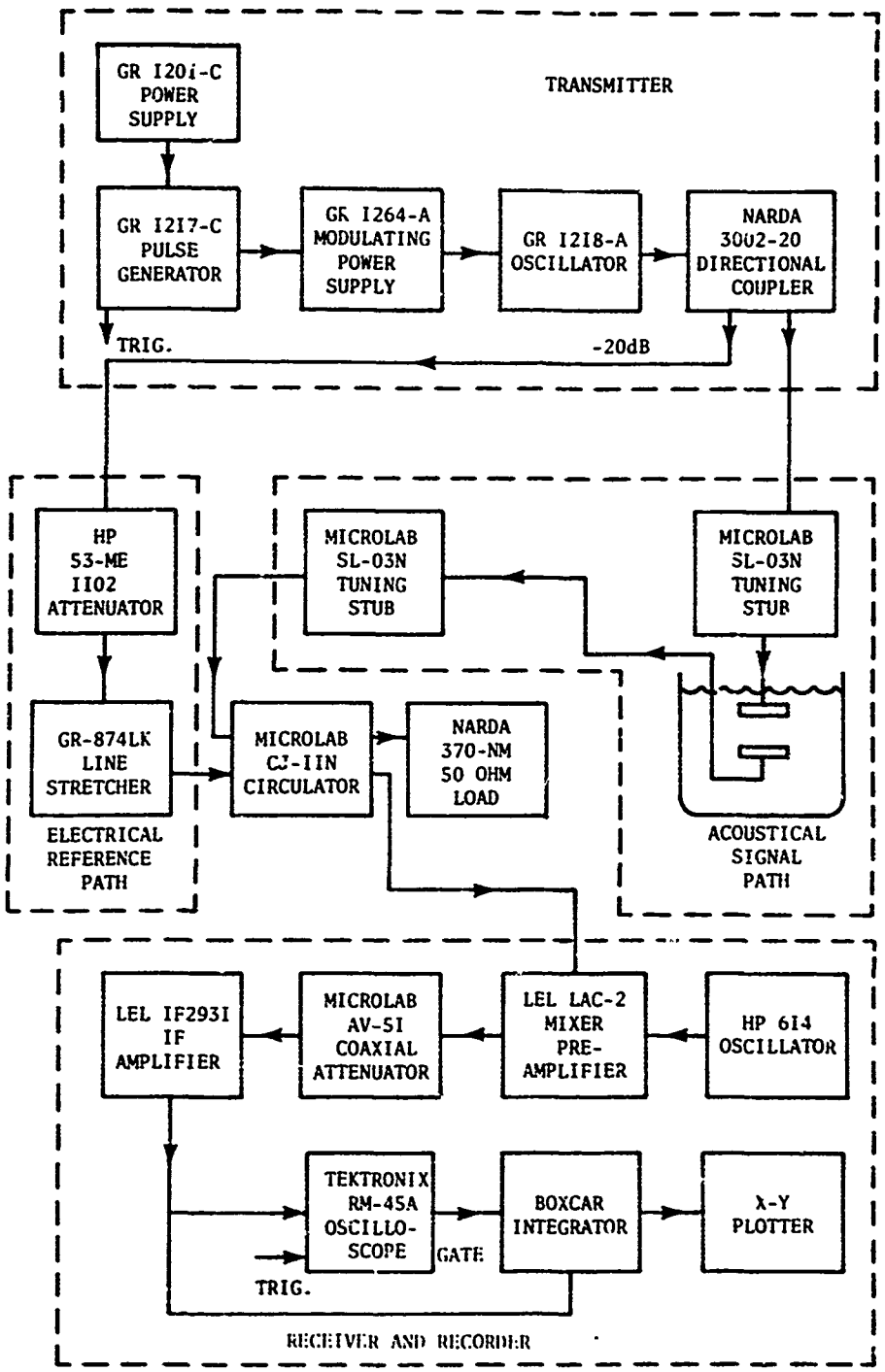

FIGURE 21.

BLOCK-DIAGRAM OF INTERFEROMETER SYSTEM

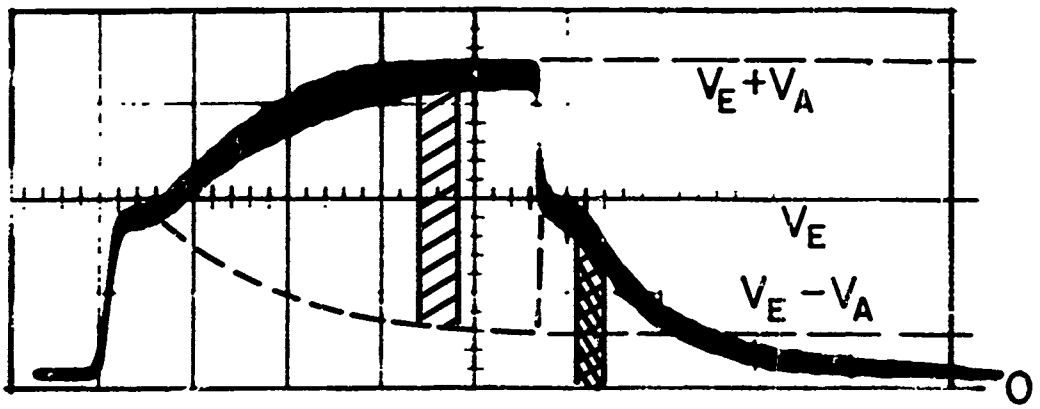

FIGURE 22.

A SCHEMATIC REPRESENTATION OF THE DEMODULATED RECEIVED SIGNAL. THE DASHED LINE INDICATES THE AREA WHICH CHANGES WHEN THE SIGNAL VARIES BETWEEN $|V_A + V_E|$ AND $|V_A - V_E|$. THE SHADED AREA IS THAT SAMPLED FOR AN ABSOLUTE ATTENUATION MEASUREMENT. THE CROSS-HATCHED AREA IS THAT SAMPLED FOR A RELATIVE ATTENUATION MEASUREMENT.

and $|V_A - V_E|$ and a signal such as the one shown in Fig. 10, could be obtained after proper processing through the box-car integrator.

The configuration of Fig. 21 could be used with the fixed path interferometer, in which case the amplitude of the signal in the cross-hatched area (Fig. 22) was sampled by the gate and the temperature of the helium was varied. This procedure gave a relative attenuation measurement, that is, a plot of the amplitude of the transmitted signal versus temperature (Fig. 23). This same result could be obtained also by using only the transmitted acoustical signal, that is, by setting the attenuator of the electrical reference path to infinity. Then the signal has no electrical component V_E and one deals only with V_A (Fig. 24).

It should be noted that by sampling the trailing portion of the received signal, the measurements were actually performed during the "off" portion of the duty cycle of the pulsed oscillator, thereby eliminating the interferences caused by electromagnetic crosstalk.

4.3.2 Temperature Drift

When the preliminary operations described above were completed, the exchange gas chamber could be pumped out to minimize the heat leak between sample chamber and helium bath. The bath was always maintained at a temperature slightly lower than the range under investigation. For the runs limited to the lambda region, 2.0°K to 2.3°K, the bath was kept at 1.95°K, typically. Heat was then provided to the sample by the heater wound around the sample chamber and the sample started to warm up. By regulating the current in the heater, one could choose the drift rate or reverse the direction of the drift. Drift rates as low as 10 m°K per

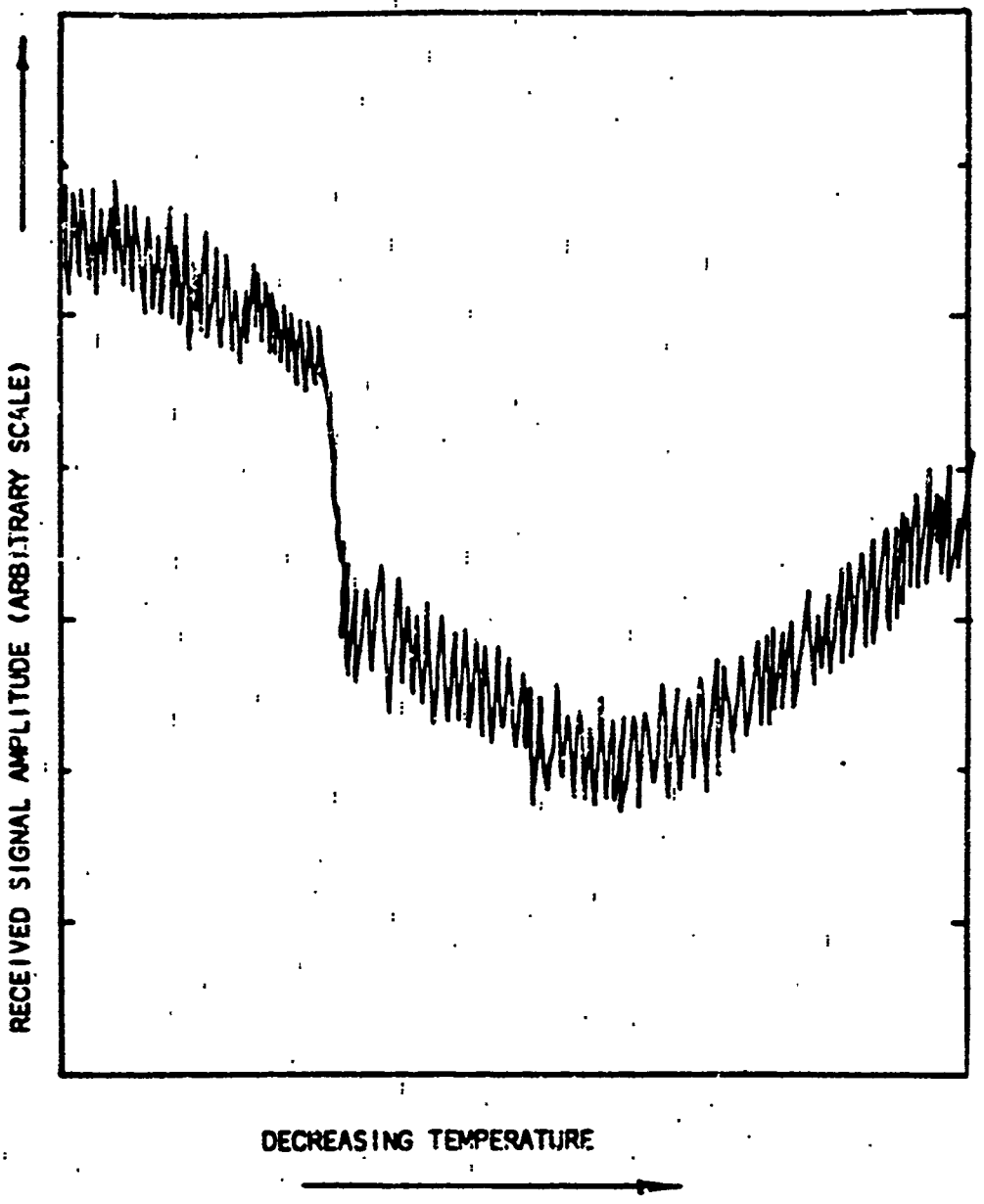

FIGURE 23.

RECEIVED SIGNAL AMPLITUDE VERSUS TEMPERATURE DURING A RELATIVE ATTENUATION MEASUREMENT. THE ABRUPT CHANGE IN SIGNAL AMPLITUDE OCCURS WHEN THE HELIUM IN THE BATH CROSSES THE LAMBDA POINT.

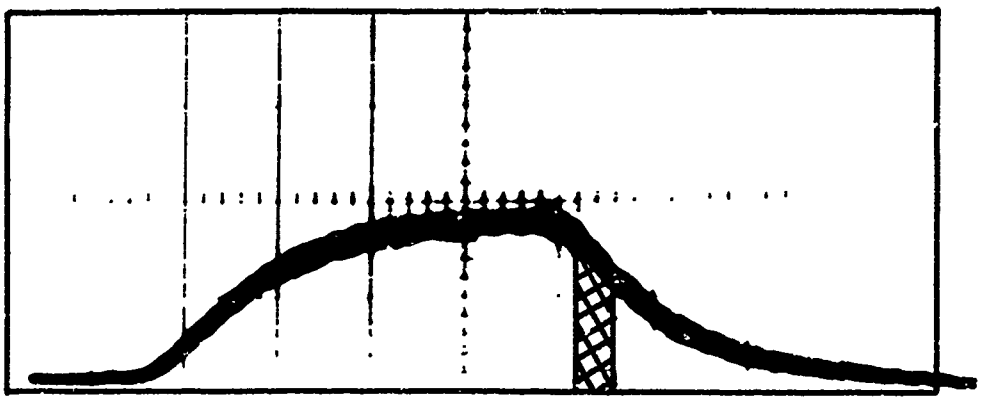

FIGURE 24.

ACOUSTICAL SIGNAL V_A.

THE CROSS-HATCHED AREA INDICATES THE PORTION OF THE SIGNAL SAMPLED FOR THE RELATIVE ATTENUATION MEASUREMENTS.

hour, or 3×10^{-6} °K sec^{-1} could thus be obtained.

V. RESULTS AND ANALYSIS

5.1 Absolute Attenuation Measurements

The method used for absolute measurements of the attenuation is identical to the one used previously by Imai.[26,42] At each point, the temperature of the system is stabilized and a plot, such as shown in Fig. 10, is generated. The amplitude of the signal decreases exponentially with the distance between the transducers. A semi-logarithmic plot of the amplitude versus the number of wavelengths of displacement (Fig. 25) can be translated into an absolute attenuation by measuring its slope. The results of these measurements are shown in Fig. 26, and confirm the previous results. Three regions can be distinguished.

5.1.1 The Normal Fluid Region ($T > 2.3°K$)

In this region, the attenuation is due principally to classical shear viscosity losses and to classical thermal conductivity losses. The continuous curves labeled α_η and α_κ represent the attenuation due to these two processes, computed from the Stokes-Kirchhoff equation (Appendix A) using known values for the quantities involved.[49] As the α_{total} curve shows, the Stokes-Kirchhoff attenuation fits well the experimental points above 3°K. Below 3°K, the discrepancy can be attributed to the fact that the critical attenuation extends into the normal fluid region.

5.1.2 The Critical Region ($2°K < T < 2.3°K$)

The sharp peak in attenuation occurring in the vicinity of the

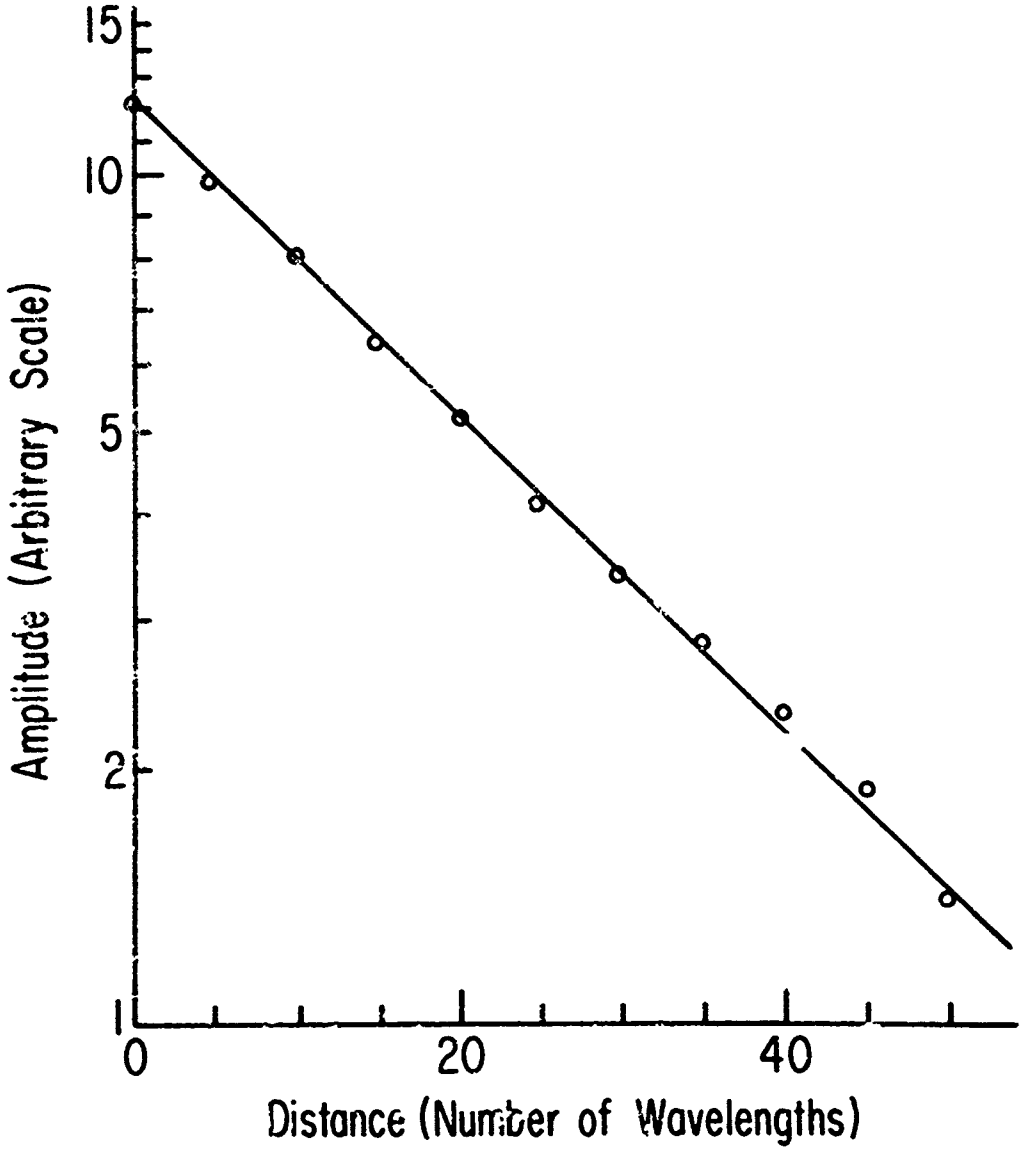

FIGURE 25.

SEMI-LOGARITHMIC PLOT OF THE RECEIVED SIGNAL AMPLITUDE VERSUS DISTANCE. ONLY EVERY FIFTH WAVELENGTH IS SHOWN FOR CLARITY. THE FIT OF THE POINTS TO A STRAIGHT LINE INDICATES THE PARALLELISM OF THE SYSTEM.

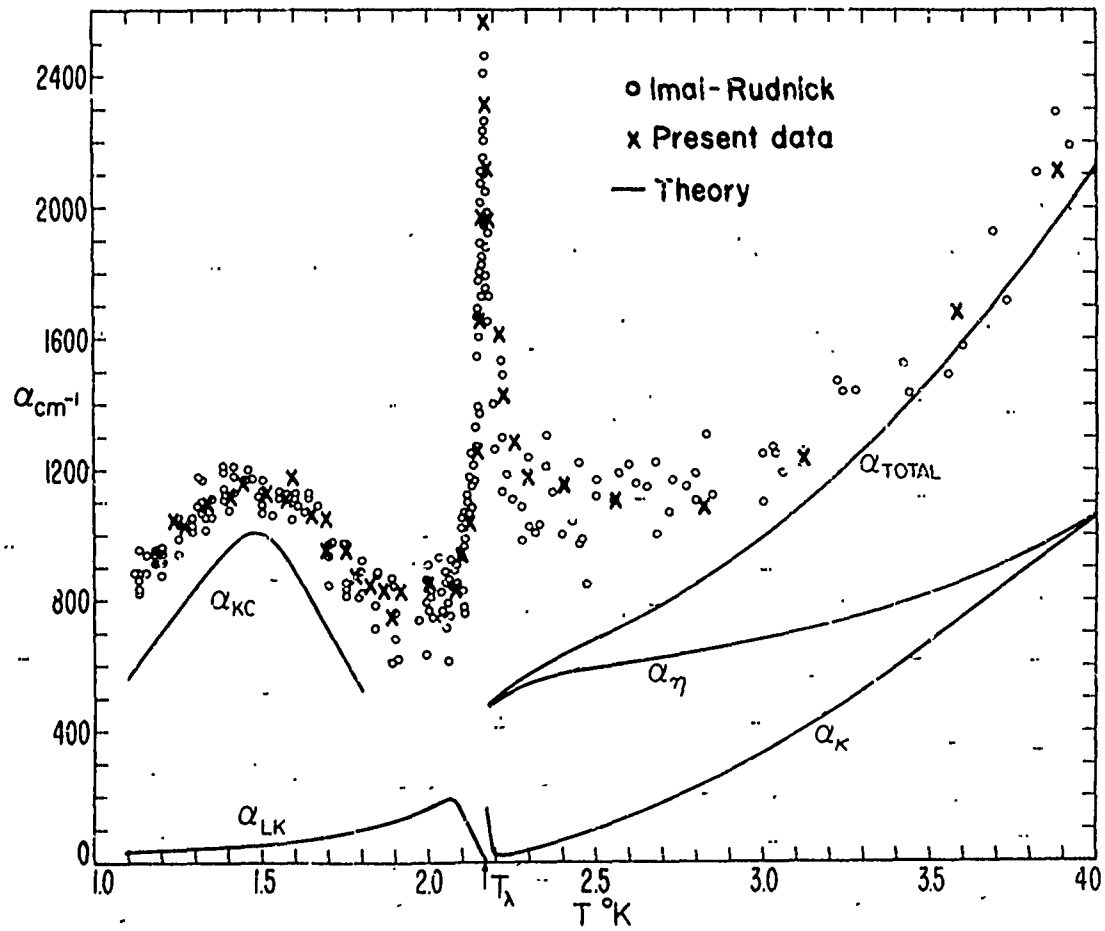

FIGURE 26.

ATTENUATION AS A FUNCTION OF TEMPERATURE IN LIQUID HELIUM AT 1 GHz.

lambda transition will be investigated in more detail in section 5.2 using a temperature drift and the fixed path interferometer. The continuous curve labeled α_{LK} is the attenuation due to the order parameter relaxation as derived in the Landau-Khalatnikov theory,[39,40] for a 1 GHz sound wave. It can be seen that this peak, which has a maximum value of 180 cm^{-1}, 94 m°K below the lambda point, represents only a small amount of the total attenuation.

5.1.3 The Superfluid Region ($T < 2°K$)

In this region, the attenuation goes through a maximum of 1200 cm^{-1} at 1.5°K, approximately. The total attenuation can be attributed to two processes:

a) The Landau-Khalatnikov α_{LK} attenuation mentioned earlier.

b) The peak in attenuation, α_{KL}, described by Khalatnikov and Chernikova,[50] which is associated with the relaxation times for equilibrium of the elementary excitations. This includes the attenuation due to classical viscosity losses (Appendix B).

As can be seen in Fig. 26, the agreement with the experimental points is good.

The location of the Khalatnikov-Chernikova peak and its shape show good agreement, except for the low temperature slope, when compared to some results obtained by Brillouin scattering by Woolf, et al.,[27] and by Heinicke, et al.[28] (Fig. 27). Compared to the results of St. Peters, et al.,[29] obtained also by Brillouin scattering, the agreement is good even for the low temperature slope. Since all those measurements were obtained at different frequencies, ranging from 556 MHz to

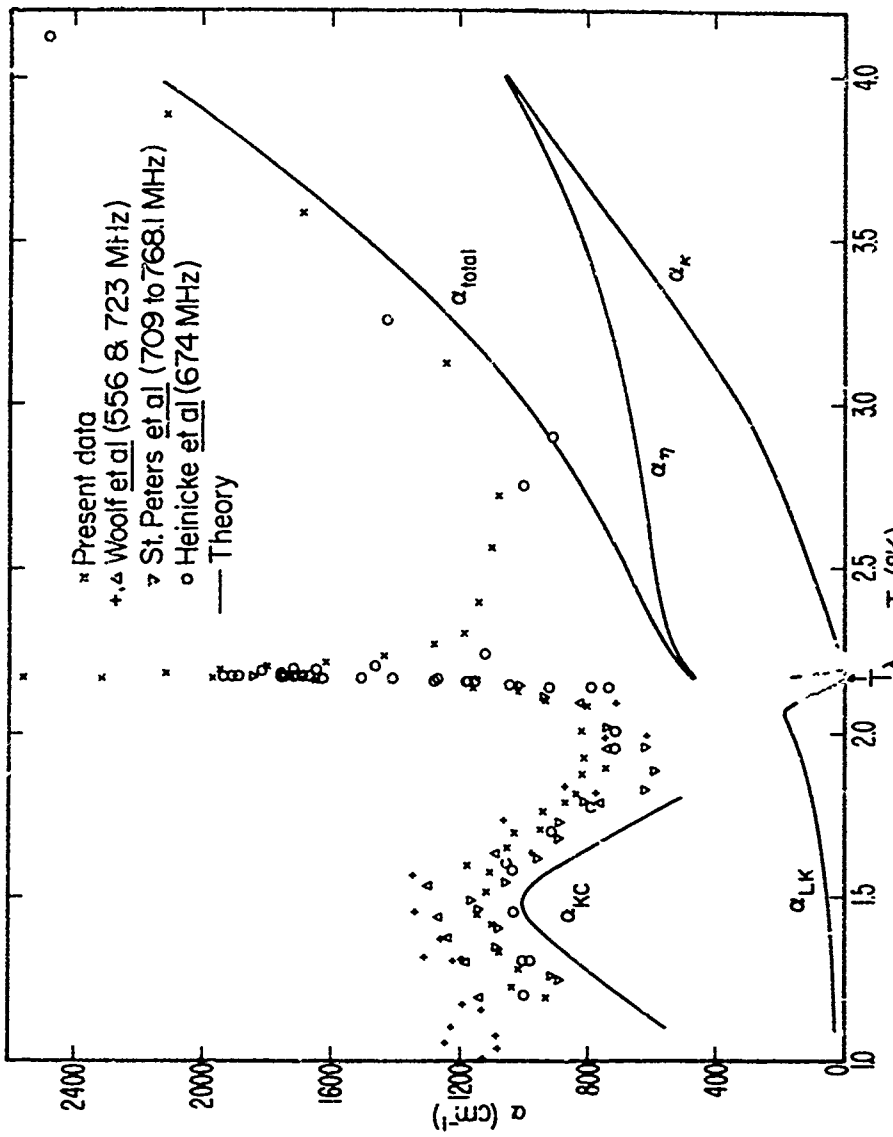

FIGURE 27.
COMPARISON BETWEEN THE PRESENT DATA AND BRILLOUIN SCATTERING DATA.

768.1 MHz, the experimental data shown in Fig. 27 has been normalized to a frequency of 1 GHz, the scaling factor being proportional to ω^2. The good agreement between most of the data points over the whole temperature range indicates that the attenuation actually scales as ω^2 with the possible exception of the lambda point region, where few points are available, and of the region below 1.5°K, where α might scale differently. It should be noted, however, that, even if it is the case, a disagreement still exists between the low temperature slope exhibited by the data of Woolf, et al., and Heinicke, et al., and the data of St. Peters, et al., and the present data.

5.2 Relative Attenuation Measurements in the Critical Region

In the critical region (2°K < T < 2.3°K) the fixed path interferometer described in Chapters III and IV was used. While the temperature of the sample was allowed to drift slowly, a simultaneous recording of the received signal amplitude and of the temperature was made (Fig. 28).

The amplitude and the attenuation are related through the equation

$$A = A_o e^{-\alpha \delta} \tag{21}$$

which expresses the spatial attenuation over an acoustical path δ, which is here the fixed gap between the transducers. The quantity A_o is also a constant of the system for each run. Equation (21) can be rewritten

$$\ln A = \ln A_o - \alpha \delta \tag{22}$$

To calibrate the relative attenuation, the absolute values obtained earlier (Fig. 26) were used; for each T, ℓn A is plotted against the

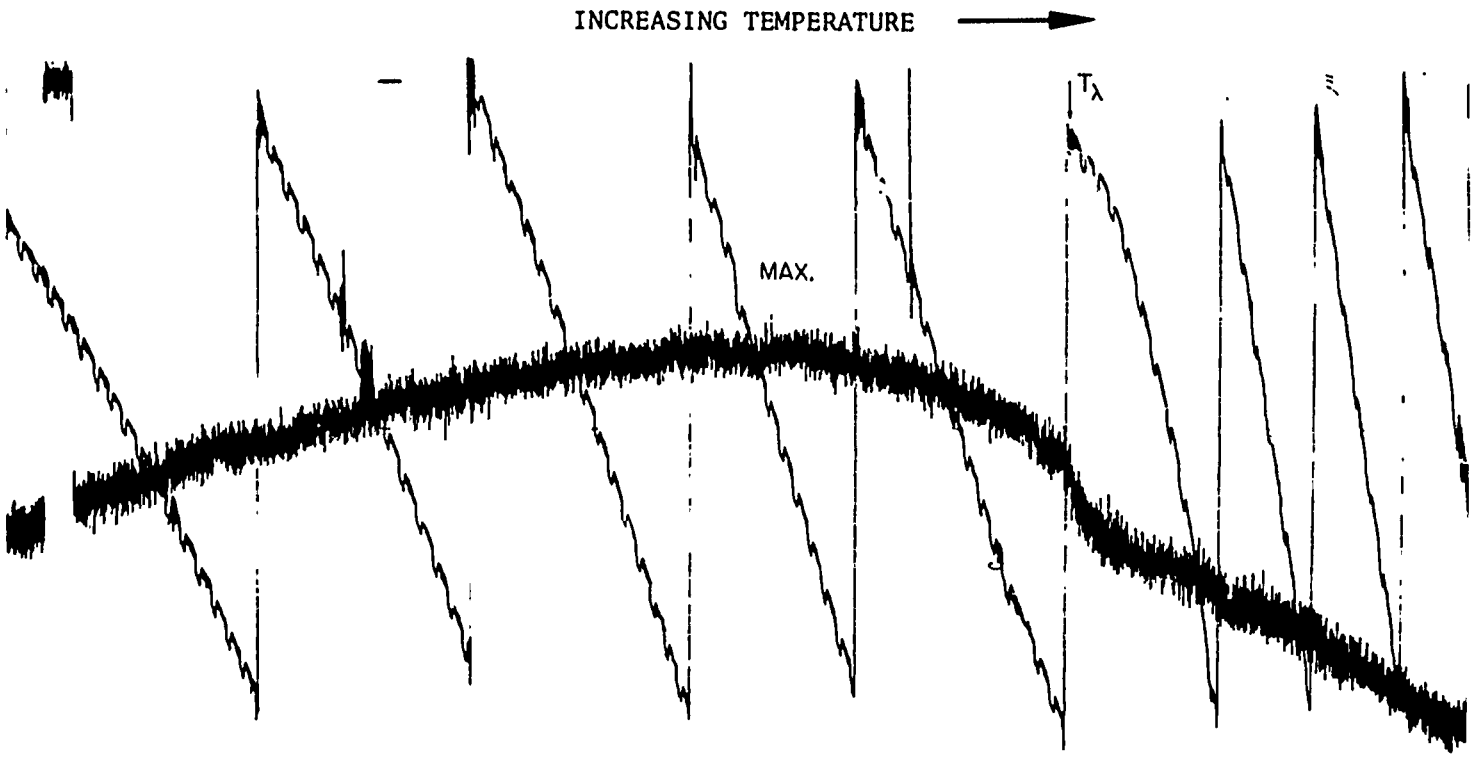

FIGURE 28.

SIMULTANEOUS RECORDING OF THE RECEIVED AMPLITUDE SIGNAL (THICK LINE) AND OF THE TEMPERATURE (THIN LINE)

absolute value of α, taking into account the experimental scattering. This procedure is shown in Fig. 29. The best straight line fitting through these points gives the scaling factor. The best value of δ for twenty runs, was found to be 1.86×10^{-3} cm which is compatible with the thickness of the spacers which was 0.75 ± 0.05 mil ($1.91 \times 10^{-3} \pm 0.13 \times 10^{-3}$ cm). The separation between the crystals is expected to be slightly greater than the actual thickness of the spacers.

For each run, the value of A_o, which depends on the input power, can be determined by extending the plot ℓn A versus α_{abs}; the intercept with the $\alpha_{abs} = 0$ axis gives $\ell n\ A_o$.

The temperature measured is that of the sample itself, the thermometer being located 7 mm from the center of the transducers and at the level of the gap.

5.2.1 Experimental Results

The outcome of these measurements is displayed in Fig. 30; typical data points are shown and the continuous line is the best fit curve for ten experimental runs. There is no singularity near the lambda transition and the absorption maximum is shifted to a temperature T_p lower than T_λ. The average of the maximum value of the attenuation is 2470 cm^{-1}. To separate that part of the attenuation which involves directly critical phenomena, and which will be called critical attenuation, the contribution of classical losses associated with the shear viscosity and thermal conductivity had to be subtracted from the total attenuation.[49] The result is shown in Fig. 31. For $T > T_\lambda$ both the shear viscosity and thermal conductivity losses have been taken into account;

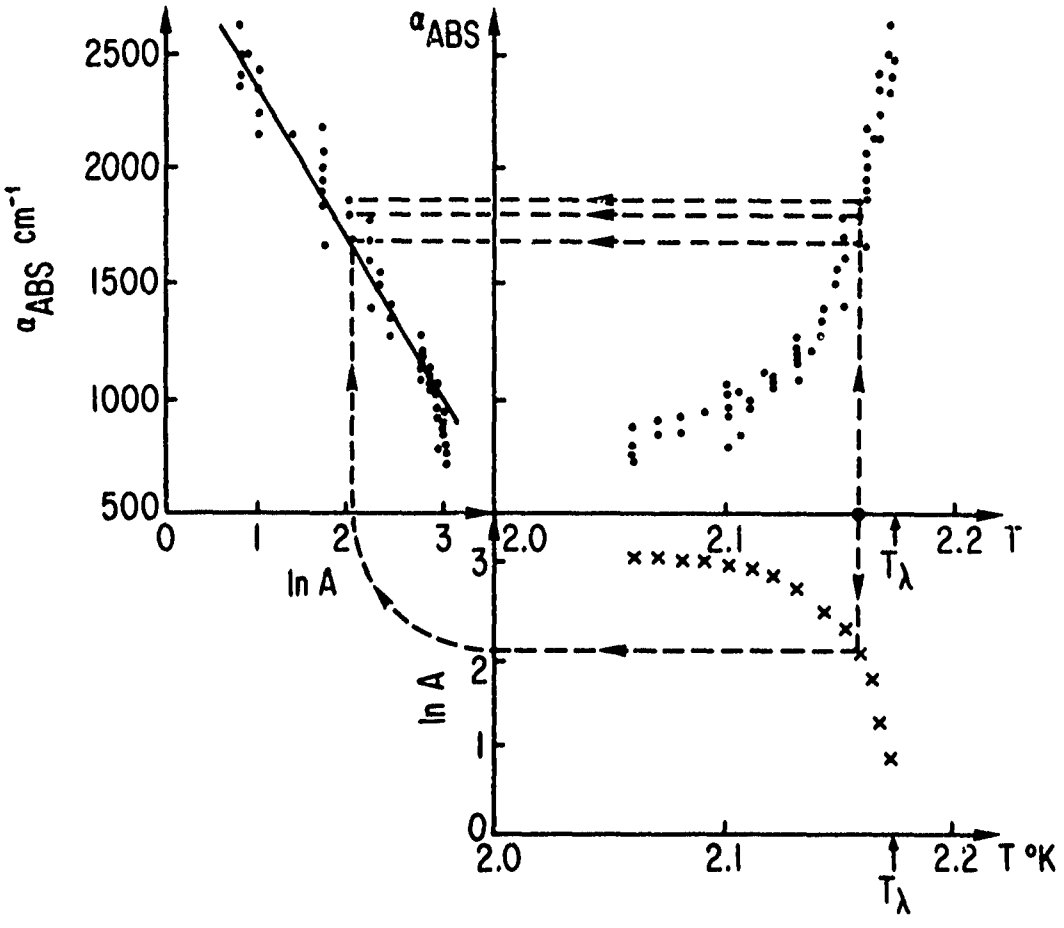

FIGURE 29.

PROCEDURE TO DETERMINE THE ATTENUATION FROM AMPLITUDE MEASUREMENTS

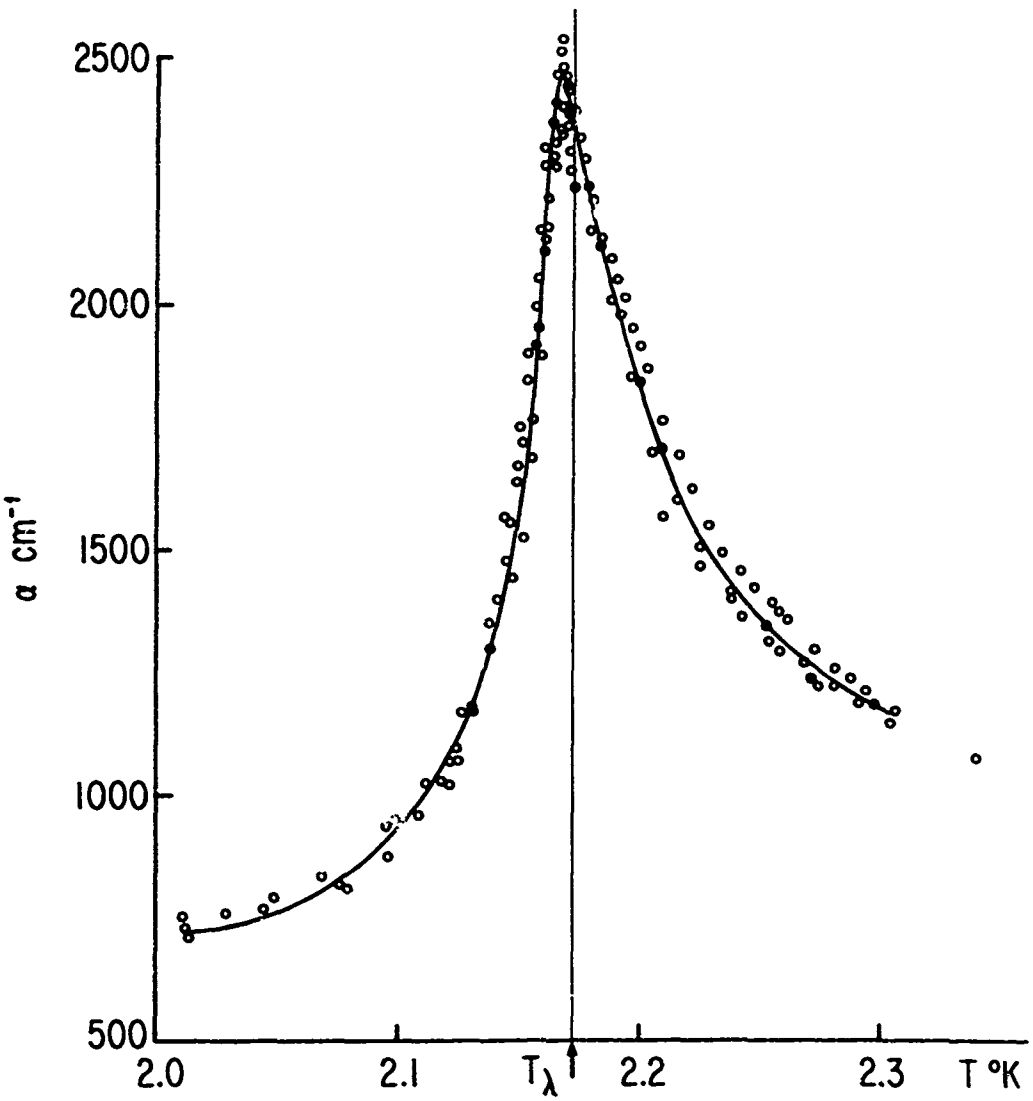

FIGURE 30.

TOTAL ULTRASONIC ATTENUATION NEAR T_λ.

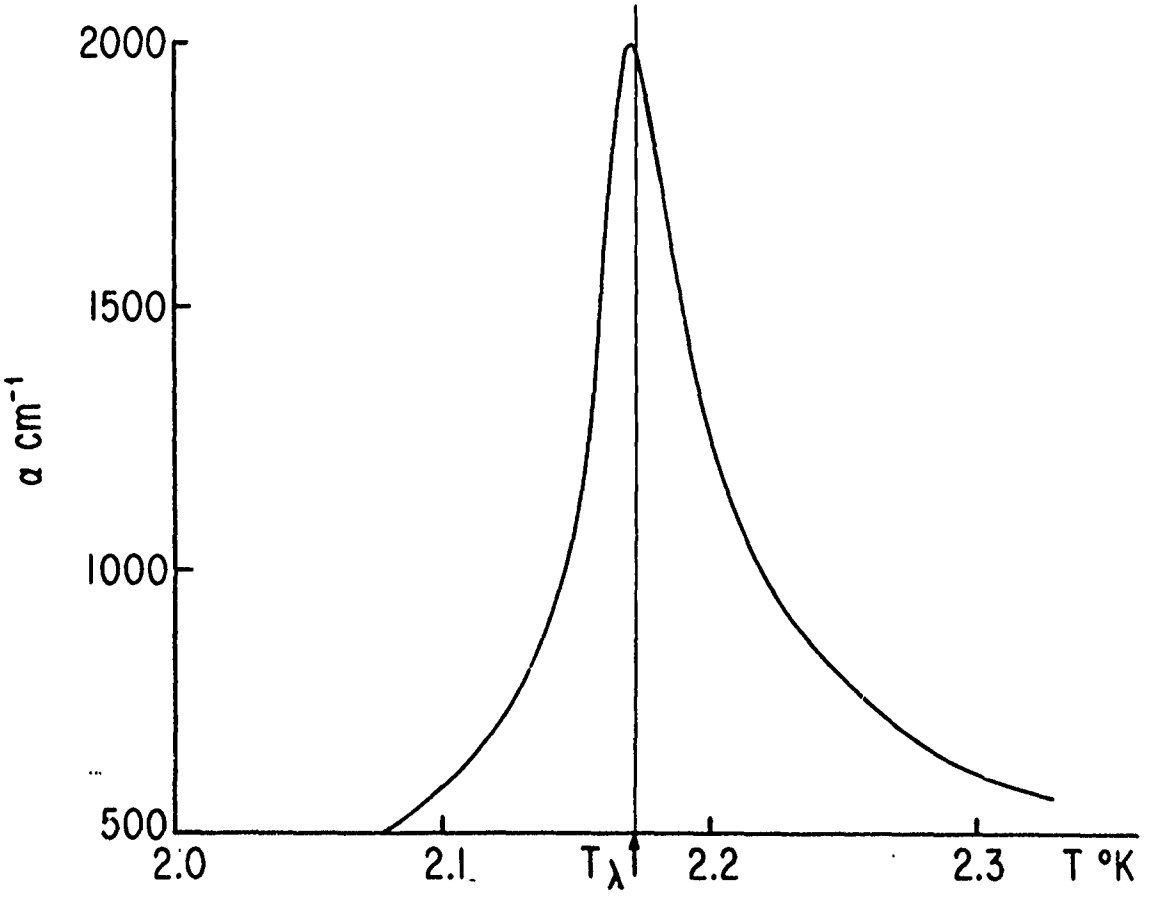

FIGURE 31.

CRITICAL ATTENUATION NEAR T_λ.

for $T < T_\lambda$ only the viscosity is available. The critical attenuation has a maximum value of about 2000 cm^{-1}.

To determine accurately the temperature T_p at which the attenuation reaches its peak value, a large number of very slow temperature drifts across the transition were performed. Drift rates as slow as 3×10^{-6} °K sec^{-1}, upward as well as downward, were reached. The amplitude of the input signal was changed from run to run and the pulse repetition frequency was varied between 1 and 300 pulses per second. No significant shift in T_p could be observed. A semi-logarithmic plot of the total attenuation versus $|T-T_\lambda|$ is shown in Fig. 32.

Eleven runs were used for the determination of the peak temperature T_p; its average value was found to be 3.26 ± 0.20 millidegrees below the lambda point.

The temperature dependence of the critical attenuation can now be investigated. Since the variations of the critical attenuation are large compared to those of the classical attenuation, subtracting the classical attenuation does not change significantly the temperature T_p of the maximum. The temperature dependence can be approximated by a power law of the form

$$\alpha = \frac{a}{|T - T_p|^n} \qquad (23)$$

In order for the fitted curve not to diverge, only the data points lying in a region $|T_p-0.02| < T < |T_p-0.125|$°K were considered. The average values for the exponent n and the coefficient a were found to be

$T > T_\lambda$ $\quad \bar{n} = 0.49 \pm 0.06 \quad \bar{a} = 232(°K) \cdot n/cm$

$T < T_\lambda$ $\quad \bar{n} = 0.51 \pm 0.05 \quad \bar{a} = 152(°K)\ n/cm$.

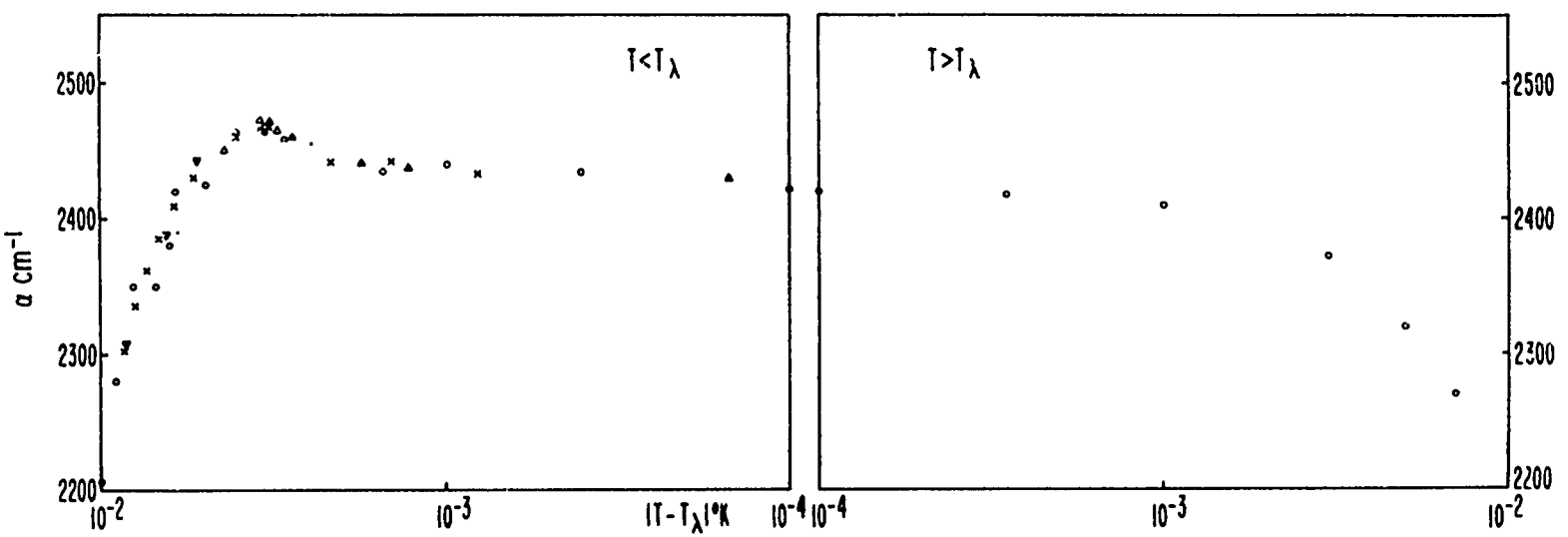

FIGURE 32.

SEMI-LOGARITHMIC PLOT OF THE TOTAL ATTENUATION vs. $|T - T_\lambda|$

The values of $\bar{n}$ given by Imai[26] are $\bar{n} = 0.46$ for $T > T_\lambda$ and $\bar{n} = 0.48$ for $T < T_\lambda$ and were computed by a function identical to (23) where T_p was $T_\lambda - 0.003$ °K.

5.2.2 Analysis and Interpretation

The present results confirm those obtained earlier in this laboratory.[26] The conditions under which the experiments were conducted at the time, namely, the fact that a submillidegree accuracy could not be achieved, made it impossible to pinpoint the temperature of the maximum in attenuation; it could only be located between 3 and 4 m°K from the transition. The present results therefore add accuracy to this result by indicating that T_p is 3.26 ± 0.20 m°K below T_λ.

First sound attenuation measurements in liquid helium at frequencies from 0.6 to 3.17 MHz[25] have also shown that the temperature at which the maximum occurs is below T_λ and the absorption has been interpreted as being due to two phenomena: (1) a relaxation process occurring only below T_λ,[40] and having a relaxation time $\tau_2 = \xi/u_2$ where u_2 is the velocity of second sound and ξ a coherence length of magnitude $1.36 \times 10^{-8} (T_\lambda - T)^{-2/3}$ cm; (2) a critical attenuation which is symmetric about T_λ, non-singular and due to fluctuations of the order parameter.

The sharp attenuation maximum occurring at about 3.3 millidegrees below T_λ cannot be explained by those two mechanisms. A relaxation peak due to a relaxation time $\tau_2 = \xi/u_2$ as above would reach a maximum of about 180 cm^{-1}, 94 millidegrees below T_λ, as shown in Fig. 26, and therefore is not a significant contribution at 1000 MHz.

On the other hand, the symmetrical attenuation peak centered at T_λ

is worthy of consideration. As shown in Fig. 33, the low frequency values of α_λ, that is, the attenuation at the lambda transition, when extrapolated to a frequency of 1 GHz, is in satisfactory agreement with the experimental results. The value of the attenuation at the transition is found to vary as $\omega^{1.22}$ from 16.8 KHz to 1 GHz as reported earlier by Williams.[25] This result agrees reasonably with those obtained by Kawasaki[36] using the mode-mode coupling theory and those of Khalatnikov, et al., resulting from a study of dynamic phenomena in a weakly interacting Bose gase, which in both cases find that the attenuation is proportional to $\omega\varepsilon^0$ in the region $\omega\tau >> 1$.

If the presence of a highly symmetrical peak, centered at T_λ, is confirmed by the theory, for the high-frequency sound waves considered here, the excess attenuation which shifts the attenuation maximum to 3.3 millidegrees below the lambda point suggests that a relaxation time, other than τ_2, manifests itself at 1 GHz.

This might indicate that, since for this very high frequency the quantity $k\xi$ does not remain small, the decay of the first sound wave into other first sound modes becomes significant, as suggested by Hohenberg.[37]

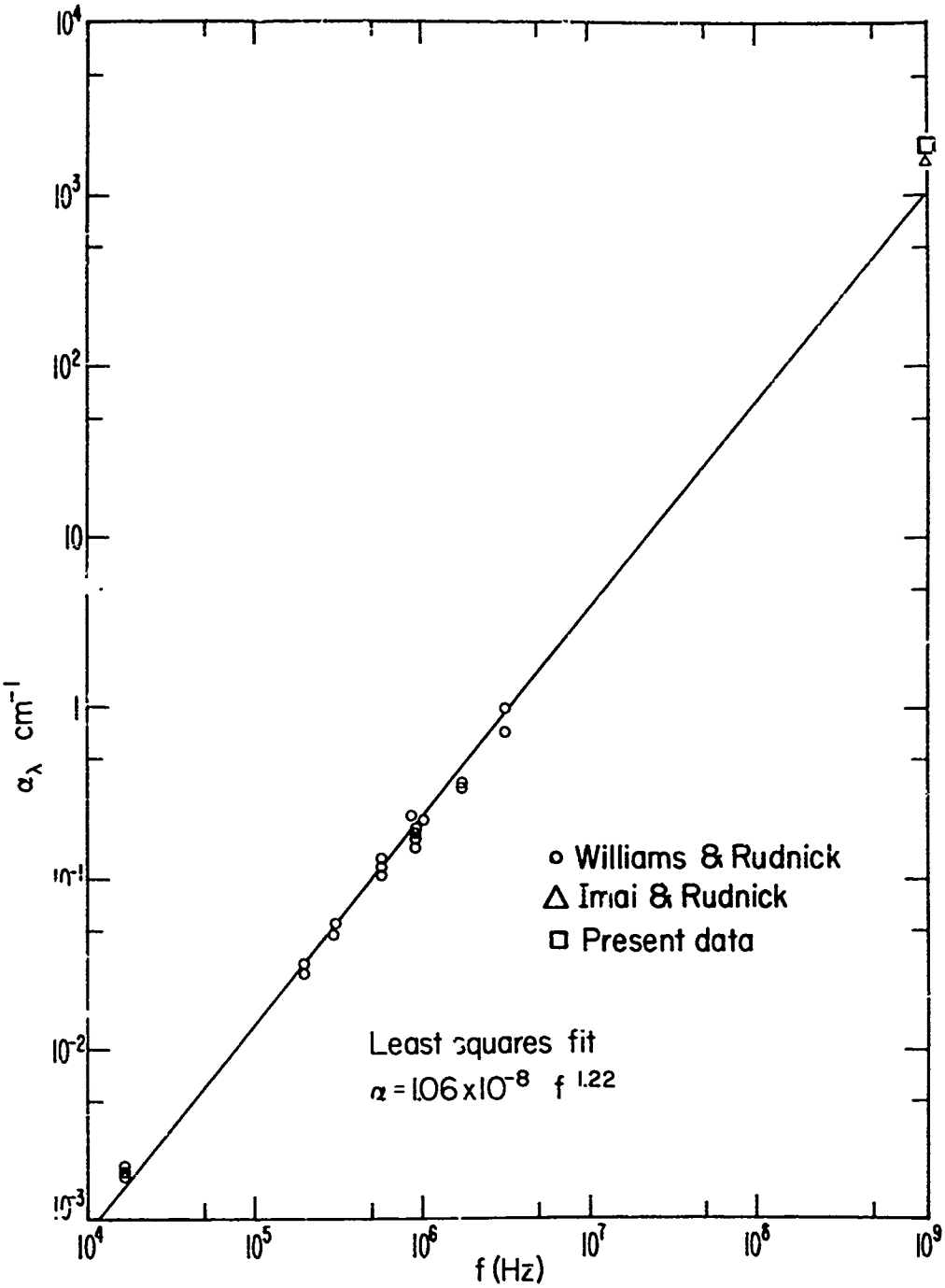

FIGURE 33.

ATTENUATION AT T = T_λ vs. FREQUENCY.

VI. CONCLUSIONS

The first part of this experiment, consisting in measuring the attenuation of 1 GHz sound waves with a variable path interferometer, from 1°K to 4°K, confirms the results obtained before by the same method and those obtained by the Brillouin scattering method. It is found that the attenuation scales as the square of the frequency over the whole temperature range, with the possible exception of data below 1.5°K and in the immediate vicinity of T_λ.

In a second part, the attenuation at 1 GHz has been measured with a fixed path interferometer in the region of the lambda transition between 2°K and 2.3°K. The sharp attenuation peak, in the critical region, is found to occur at 3.26 ± 0.20 m°K below T_λ. The maximum value of the attenuation is close to 2500 cm^{-1}.

After the contribution of viscous and thermal losses to the attenuation has been subtracted, the temperature dependence of the critical attenuation is found to be approximately $|T_p-T|^{-1/2}$ on both sides of T_p, the temperature of the peak, excluding the immediate neighborhood of T_p.

Since the contribution of the Landau-Khalatnikov mechanism to the attenuation at a frequency of 1 GHz is only about 180 cm^{-1} at its maximum, which occurs 94 millidegrees below T_λ, the large absorption is due to other processes. The existing theories of first sound attenuation in liquid helium have been surveyed and no satisfactory explanation of the sharp attenuation peak in the vicinity of T_λ has been found.

VII. SUGGESTED EXPERIMENTS

In order to reach a better understanding of attenuation phenomena in the lambda transition region, the following experiments would be of interest:

1) The gap existing between the present results and those obtained at low frequencies should be narrowed. Measurements between 4 MHz and 1000 MHz would be useful. A good knowledge of the relaxation times involved will come from frequency dependent data.

2) Measurements of the attenuation under different pressures (including high pressure) would provide an interesting evaluation of the Pokrovskii-Khalatnikov theory.[40]

3) Finally, measurements over the whole frequency range, in mixtures of He^4 and He^3 and in other substances undergoing an order-disorder lambda transition, will lead to interesting comparisons and generalizations.

BIBLIOGRAPHY

1. E. C. Kerr and R. D. Taylor, Ann. Phys. (N.Y.) 26, 292 (1964).

2. W. H. Keesom and K. Clusius, Proc. Roy. Acad. Amsterdam 35, 307 (1932); Leiden Commun. 219e; W. H. Keesom and A. P. Keesom, Proc. Roy. Acad. Amsterdam 35, 736 (1932); Leiden Commun. 221d.

3. M. J. Buckingham, W. M. Fairbank, and C. F. Keller, Proc. 5th Int. Conf. Low Temp. Phys., Madison, Wisconsin (1957), p. 50.

4. L. Tisza, Compt. Rend. 207, 1035 (1938).

5. V. Peshkov, J. Phys. (USSR) 10, 389 (1946).

6. K. R. Atkins, Phys. Rev. 113, 962 (1959).

7. C. W. F. Everitt, K. R. Atkins, and A. Denenstein, Phys. Rev. Letters 8, 161 (1962); Phys. Rev. 136, A1494 (1964).

8. J. R. Pellam, Phys. Rev. 73, 608 (1948).

9. I. Rudnick and K. A. Shapiro, Phys. Rev. Letters 9, 191 (1962); K. A. Shapiro and I. Rudnick, Phys. Rev. 137, A1383 (1965).

10. L. Tisza, J. Phys. Radium 1, 164 (1940); 1, 350 (1940).

11. P. Kapitza, Nature 141, 74 (1938).

12. J. F. Allen and A. D. Misener, Nature 141, 75 (1938).

13. W. H. Keesom and J. E. MacWood, Physica 5, 737 (1938).

14. R. G. Hussey, B. J. Good, and J. M. Reynolds, Phys. Fluids 10, 89 (1967).

15. W. E. Keller, Helium-3 and Helium-4 (Plenum Press, New York, 1969); K. R. Atkins, Liquid Helium (University Press, Cambridge, 1959); J. Wilks, The Properties of Liquid and Solid Helium (Clarendon Press, Oxford, 1967).

16. L. D. Landau and E. M. Lifshitz, Statistical Physics (Addison-Wesley Publ. Co., Reading, Mass., 1958).

17. Leo P. Kadanoff, Wolfgang Götze, David Hamblen, Robert Hecht, E. A. S. Lewis, V. V. Palciauskas, Martin Rayl, J. Swift, David Aspnes, and Joseph Kane, Rev. Mod. Phys. 39, 395 (1967).

18. B. Widom, J. Chem. Phys. 43, 3892 (1965); 43, 3898 (1965).

19. R. A. Ferrell, N. Menyhàrd, H. Schmidt, F. Schwabl, and P. Szépfalusy, Ann. Phys. (N.Y.) 47, 565 (1968).

20. B. I. Halperin and P. C. Hohenberg, Phys. Rev. Letters 19, 700 (1967); Phys. Rev. 177, 952 (1968).

21. C. W. Garland, Physical Acoustics, W. P. Mason and R. N. Thurston, eds., Vol. VII, Chap. 2 (Academic Press, New York, 1970).

22. J. R. Pellam and C. F. Squire, Phys. Rev. 72, 1245 (1947).

23. C. E. Chase, Phys. Fluids 1, 193 (1958).

24. M. Barmatz and I. Rudnick, Phys. Rev. 170, 224 (1968).

25. D. Williams and I. Rudnick, Phys. Rev. Letters 25, 276 (1970).

26. J. S. Imai and I. Rudnick, Phys. Rev. Letters 22, 694 (1969).

27. M. A. Woolf, P. M. Platzman, and M. G. Cohen, Phys. Rev. Letters 17, 294 (1966); M. G. Cohen and I. E. Gordon, IEEE J. Quantum Electron. QE2, 8A-8 (1966).

28. W. Heinicke, G. Winterling, and K. Dransfeld, Phys. Rev. Letters 22, 170 (1969).

29. R. L. St. Peters, T. J. Greytag, and G. B. Benedek, Opt. Commun. (Neth.) 1, 412 (1970).

30. B. Golding and M. Barmatz, Phys. Rev. Letters 23, 223 (1969).

31. V. L. Ginzburg, Dokl. Akad. Nauk SSSR 105, 240 (1955).

32. A. P. Levanyuk, Soviet Phys.-JETP 22, 901 (1966).

33. D. Stauffer and Victor K. Wong, J. Low Temp. Phys. 2, 599 (1970).

34. L. P. Kadanoff, Physics 2, 263 (1966).

35. Victor K. Wong, Phys. Letters 29A, 441 (1969).

36. K. Kawasaki, Phys. Letters 31A, 165 (1970); Phys. Rev. A3, 1097 (1971).

37. P. C. Hohenberg, Varenna Summer School on Critical Phenomena (Preprint).

38. I. M. Khalatnikov, V. L. Pokrovskii, and D. M. Semiz, J. Low Temp. Phys. 6, 305 (1972).

39. L. D. Landau and I. M. Khalatnikov, Dokl. Akad. Nauk SSSR 96, 469 (1954).

40. V. L. Pokrovskii and I. M. Khalatnikov, JETP Letters 9, 149 (1969); I. M. Khalatnikov, Soviet Phys.-JETP 30, 268 (1970).

41. L. D. Landau and I. M. Lifshitz, Fluid Mechanics (Addison-Wesley Publ. Co., Reading, Mass., 1959).

42. J. S. Imai, Doctoral Dissertation, Department of Physics, University of California, Los Angeles (1969).

43. V. P. Peshkov, K. N. Zinoveva, and A. I. Filimonov, Soviet Phys.-JETP 9, 734 (1959).

44. M. Barmatz, Doctoral Dissertation, Department of Physics, University of California, Los Angeles (1966).

45. D. Berlincourt, H. Jaffe, and L. R. Shiozawa, Phys. Rev. 129, 1009 (1963).

46. D. Beecham, Ultrasonics 5, 19 (1967).

47. D. W. Robinson, Doctoral Dissertation, University of California, Los Angeles (1971).

48. J. deKlerk and E. F. Kelly, Rev. Sci. Instr. 36, 506 (1965).

49. G. Ahlers, Phys. Rev. Letters 21, 1159 (1968); C. E. Chase, Proc. Royal Soc. A220, 116 (1953); C. Grenier, Phys. Rev. 83, 598 (1951); R. W. Hill and O. V. Louanasmaa, Phil. Mag. 2, 143 (1957); E. C. Kerr, J. Chem. Phys. 26, 511 (1957); E. C. Kerr and R. D. Taylor, Ann. Phys. (N.Y.) 26, 292 (1964); R. D. Taylor and J. G. Dash, Phys. Rev. 106, 398 (1957); H. Van Dijk, M. Durieux, J. R. Clement, and J. K. Logan, N.B.S. Monograph 10, 1958 Scale of Temperature (1960); M. Archibald, J. M. Mochel, and L. Weaver, Phys. Rev. Letters 21, 1156 (1968).

50. I. M. Khalatnikov and D. M. Chernikova, Soviet Phys.-JETP 22, 1336 (1966); 23, 274 (1966); JETP Letters 2, 351 (1965).

51. A. M. Polyakov, Soviet Phys.-JETP 30, 1164 (1970).

52. W. M. Whitney and C. E. Chase, Phys. Rev. 158, 200 (1967).

APPENDIX A

THE STOKES-KIRCHHOFF EQUATION

The classical attenuation of sound in an ordinary liquid is given by the Stokes-Kirchhoff equation

$$\alpha = \frac{\omega^2}{2\rho u_1^3}\left(\frac{4}{3}\eta + \zeta + \frac{\gamma-1}{\gamma}\frac{K}{C_v}\right) \tag{24}$$

where ω is the angular frequency, ρ the density, u_1 the velocity of (first) sound, η the shear viscosity, ζ the volume viscosity, γ the ratio of the specific heats, κ the heat conductivity, and C_v the specific heat at constant volume.

To compute the last term of this equation, which represents the absorption due to thermal losses, it must be expressed in terms of quantities measured[49] at the saturated vapor pressure:

$$\alpha_\kappa = \frac{\omega^2}{2\rho u_1^3}\frac{\gamma-1}{\gamma}\frac{K}{C_v} \tag{25}$$

Using the following relations:

$$\gamma - 1 = \frac{TV\beta_P^2}{K_T C_v} \tag{26}$$

$$\beta_P = \frac{\beta_{sat} + \left(\frac{\partial P}{\partial T}\right)_{sat}\frac{1}{\rho u_1^2}}{1 - \frac{TV}{C_s}\left(\frac{\partial P}{\partial T}\right)_{sat}\left[\beta_{sat} + \left(\frac{\partial P}{\partial T}\right)_{sat}\frac{1}{\rho u_1^2}\right]} \tag{27}$$

$$C_p = \frac{C_s}{1 - \frac{TV}{C_s}\left(\frac{\partial P}{\partial T}\right)_{sat}\left[\beta_{sat} + \left(\frac{\partial P}{\partial T}\right)_{sat}\frac{1}{\rho u_1^2}\right]} \tag{28}$$

this term reduces to:

$$\alpha_K = \frac{\omega^2 K T V}{2 u_1 C_s^2} \left[\beta_{sat} + \left(\frac{\partial P}{\partial T} \right)_{sat} \frac{1}{\rho u_1^2} \right]^2 \qquad (29)$$

where β_p is the isobaric coefficient of thermal expansion, C_p is the specific heat at constant pressure, K_T is the isothermal compressibility. The subscript "sat." indicates that a quantity is evaluated at the saturated vapor pressure.

APPENDIX B

THE KHALATNIKOV-CHERNIKOVA THEORY

The Khalatnikov-Chernikova theory of the absorption of sound in superfluid helium states that the interactions of elementary excitations (phonons and rotons) cause many mechanisms of energy dissipation. To each of those mechanisms is associated a relaxation time τ characteristic of the amount of time required for the distributions of elementary excitations to adjust to the disturbance created by the sound wave. Some processes do not contribute significantly to the attenuation because their relaxation time is very short; such is the case for the elastic scattering of phonons by phonons and for the roton-roton scattering processes. Some other processes, by their relatively long relaxation times, contribute to the attenuation; such are the interactions which involve the conversion of a phonon into a roton, to which is associated a relaxation time τ_{pr}, or the conversion of three phonons into two, the five-phonon process to which is associated a relaxation time $\tau_{3\to2}$.

The expression for the attenuation of first sound can be simplified in the high temperature region, above 1.2°K, for which the only case of interest is $\omega\tau_{pr} \ll 1$. In the notation of Whitney[52]

$$\alpha(\omega,T) = \frac{\omega^2 \tilde{\tau}_{pr}}{u_1} \left(\frac{\rho_n}{\rho}\right) \left[\frac{2}{15} + \frac{1}{c^3} (3u+1)^2\right] \qquad (30)$$

with

$$\tilde{\tau}_{pz} = \tau_{pz}\left[1 + \frac{.376}{.451\frac{\tau_{pz}}{\tau_{3\to 2}} + .0036}\right] \tag{31}$$

$$\frac{1}{\beta} = \left[\frac{1.453}{T} + \frac{\tau_{3\to 2}}{\tau_{pz}} \times .166\right]\frac{\tau_{pz}}{\tau_{3\to 2}} \tag{32}$$

where

$$\tau_{3\to 2} = 1.288 \times 10^{-8}\ T^{-9} \tag{33}$$

$$u = \frac{f}{u_1}\left(\frac{\partial u_1}{\partial f}\right) = 2.642 \tag{34}$$

$$\frac{f_n}{f} = 1.218 \times 10^{-4}\ T^{4} \tag{35}$$

$$\frac{1}{\tau_{pz}} = 1.28 \times 10^{12}\ T^{9/2}\ e^{-\frac{\Delta}{kT}} \tag{36}$$

where k is the Boltzmann constant and $\Delta = 3.4 \times 10^{43}$.

The five-phonon collision time is the adjustable parameter of this theory.

At high temperatures the relaxation times involved in the scattering processes are short compared to the period of the acoustic wave; the system is in a hydrodynamic regime. At low temperatures, on the contrary, the relaxation times are long and the system is in a collisionless regime. The two regimes are separated by an attenuation maximum. At 1 GHz this maximum occurs at 1.48°K and has an amplitude of 1012 cm^{-1}.